

Master Thesis



Universidad del País Vasco Euskal Herriko Unibertsitatea

Stimulation discomfort comparison of asynchronous and synchronous methods with multi-field electrodes

Eukene Imatz Ojanguren

Donostia - San Sebastián, May 2013

Universidad del País Vasco / Euskal Herriko
Unibertsitatea
Departamento de Ciencia de la Computación
e Inteligencia Artificial

Supervisors UPV/EHU: - Basilio Sierra
- Itziar Irigoyen

Supervisors Tecnalía: - Thierry Keller

www.ccia-kzaa.ehu.es

Acknowledgments

First and foremost, I wish to express my sincere gratitude to all my colleagues and supervisors of Tecnalía and UPV/EHU for their valuable guidance, advice and help during different stages of the project. I would also like to point out that this research project wouldn't have been possible without all the people that participated in the experiments, so I would like to express my deepest gratitude to all of them, for their participation and patience. Besides, an honorable mention goes to my family and friends for their enthusiastic support, understanding and help through the duration of this project. Finally, I want to thank Tecnalía and Fundación Iñaki Goenaga for providing me the opportunity to carry out this project.

Abstract

Functional Electrical Stimulation (FES) is a technique that consists on applying electrical current pulses to artificially activate motor nerve fibers and produce muscle contractions to achieve functional movements. The main applications of FES are within the rehabilitation field, in which this technique is used to aid recovery or to restore lost motor functions. People that benefit of FES are usually patients with neurological disorders which result in motor dysfunctions; most common patients include stroke and spinal cord injury (SCI). Neuroprosthesis are devices that have their basis in FES technique, and their aim is to bridge interrupted or damaged neural paths between the brain and upper or lower limbs. One of the aims of neuroprosthesis is to artificially generate muscle contractions that produce functional movements, and therefore, assist impaired people by making them able to perform activities of daily living (ADL).

FES applies current pulses and stimulates nerve fibers by means of electrodes, which can be either implanted or surface electrodes. Both of them have advantages and disadvantages. Implanted electrodes need open surgery to place them next to the nerve root, so these electrodes carry many disadvantages that are produced by the use of invasive techniques. In return, as the electrodes are attached to the nerve, they make it easier to achieve selective functional movements. On the contrary, surface electrodes are not invasive and are easily attached or detached on the skin. Main disadvantages of surface electrodes are the difficulty of selectively stimulating nerve fibers and uncomfortable feeling perceived by users due to sensory nerves located in the skin.

Electrical stimulation surface electrode technology has improved significantly through the years and recently, multi-field electrodes have been suggested. This multi-field or matrix electrode approach brings many advantages to FES; among them it is the possibility of easily applying different stimulation methods and techniques. The main goal of this thesis is therefore, to test two stimulation methods, which are asynchronous and synchronous stimulation, in the upper limb with multi-field electrodes. To this end, a purpose-built wrist torque measuring system and a graphic user interface were developed to measure wrist torque produced with each of the methods and to efficiently carry out the

experiments. Then, both methods were tested on 15 healthy subjects and sensitivity results were analyzed for different cases. Results show that there are significant differences between methods regarding sensation in some cases, which can affect effectiveness or success of FES.

Key-words

- Functional Electrical Stimulation
- Multi-field electrodes
- Asynchronous stimulation
- Synchronous stimulation
- Discomfort

Table of Contents

1. Introduction	1
1.1 Background.....	1
1.2 Motivation and aim	2
1.3 Thesis structure	2
2. State of the art	5
2.1 Physiology	5
2.1.1 Nervous system and nerve cells	5
2.1.2 Movement.....	9
2.1.3 Neuromuscular electrical stimulation basis.....	14
2.1.4 Clinical applications	18
2.2 Technology	20
2.2.1 Electrodes.....	21
2.2.2 Stimulators.....	25
2.2.3 Upper-limb transcutaneous neuroprosthesis	27
2.2.4 Hand kinematic and dynamic analysis systems	29
3. Materials	37
3.1 IntFES stimulation device.....	37
3.2 Wrist torque measuring set-up	39
3.3 User interface (MATLAB)	45
4. Experiments	47
4.1 Stimulation methods.....	47

4.1.1	Asynchronous stimulation	47
4.1.2	Synchronous stimulation	48
4.2	Protocol design	48
4.2.1	Torque	49
4.2.2	Discomfort.....	51
4.2.3	Cases.....	52
4.3	Procedure	53
4.3.1	Adaptation sessions	53
4.3.2	Preparation	53
4.3.3	Calibration.....	53
4.3.4	Stimulation and evaluation	55
5.	Results	57
5.1	Success	60
5.2	Discomfort.....	61
6.	Conclusions and future work	65
7.	References.....	67
8.	Acronyms	79
9.	Appendix I	81
9.1	IntFES stimulator specifications.....	81
9.2	Force sensor specifications	82
9.3	GUI description	83

List of figures

Figure 2.1 – Membrane potential on the cell membrane.....	6
Figure 2.2 – Structure of a neuron.....	8
Figure 2.3 – Different neuron types..	9
Figure 2.4 – Motor unit.	10
Figure 2.5 – Sarcomere structure.....	11
Figure 2.6 – Contractile force developed over muscle length.	12
Figure 2.7 – Active tension on the muscle for different frequencies.....	13
Figure 2.8 – NMES.....	14
Figure 2.9 – Current distribution.	15
Figure 2.10 – Different pulse configurations and tissue damage	16
Figure 2.11 – Amplitude effects.....	16
Figure 2.12 – Amplitude vs. Pulse duration.	17
Figure 2.13 – Fatigue for different frequencies..	17
Figure 2.14 – FES to restore damaged motor function.	19
Figure 2.15 – Nerves left forearm anterior view – Nerves right forearm posterior view.....	20
Figure 2.16 – Implanted electrode types: cuff, wraparound and epymisial.....	22
Figure 2.17 – Metal plate electrodes covered by fabric.....	23
Figure 2.18 – Carbon or rubber electrode.....	24
Figure 2.19 – Hydrogel electrode structure and hydrogel electrodes.....	24
Figure 2.20 – Multi-field electrode..	25
Figure 2.21 – DUO-Stim stimulator device, programmer and portable stimulator units	26
Figure 2.22 – UNAFET 8 stimulator.....	26
Figure 2.23 – Compex Motion Stimulator.	27
Figure 2.24 – NESS H200 Wireless: 1-orthosis, 2-control box.....	28

Figure 2.25 – Data driven pose estimation method: Pose database and matching.	31
Figure 2.26 – Cyberglove.	32
Figure 2.27 – Humanglove	33
Figure 2.28 – 5DT Data Glove.....	33
Figure 2.29 – DGTech VHand with reference axes.....	34
Figure 2.30 – Biodex S4 dynamometer..	35
Figure 2.31 – Example of hand-held dynamometer and grip dynamometer.	36
Figure 3.1 – IntFES stimulator.....	37
Figure 3.2 – Different IntFES array configurations.	38
Figure 3.3 – Electrode designed for forearm stimulation.....	38
Figure 3.4 – IntFES electronic board and connector of the stimulator cable.	39
Figure 3.5 – Force sensor and orientation of three axes (X,Y,Z).....	40
Figure 3.6 – Frontal view of wrist torque measuring set up.	41
Figure 3.7 – Lateral view of wrist torque measuring set up.	42
Figure 3.8 – Theoretical values compared to measurements.....	43
Figure 3.9 – MSE values for each position.	43
Figure 3.10 – Gage R&R repeatability results.....	44
Figure 3.11 – Custom made GUI (different parts marked).	45
Figure 4.1 – Asynchronous stimulation.....	47
Figure 4.2 – Synchronous stimulation.....	48
Figure 4.3 – Combination of torques produced by gravity and stiffness.	49
Figure 4.4 – Torque measured in each position with hand relaxed, flexible subject.....	50
Figure 4.5 – Torque measured in each position with hand relaxed, not so flexible subject.....	51
Figure 4.6 – 8 different cases.	52
Figure 4.7 – Subject during experiment.	54

Figure 4.8 – Pad configuration examples: 2 neighbor, 2 distant, 3 neighbor, 3 distant.	54
Figure 4.9 – Example of hand at rest and hand reaching the target.....	56
Figure 5.1 – Normalized torque vs. amplitude for 2 neighbor pads.	58
Figure 5.2 – Normalized torque vs. amplitude for 3 neighbor pads.	58
Figure 5.3 – Normalized torque vs. amplitude for 2 distant pads.	59
Figure 5.4 – Normalized torque vs. amplitude for 3 distant pads.	59
Figure 5.5 – Number of successes detailed.....	60
Figure 5.6 – Number of successes.	61
Figure 5.7 – Discomfort means and standard deviation intervals detailed.	62
Figure 5.8 – Discomfort means and standard deviation intervals.....	62
Figure 5.9 – Superficial discomfort rates.	63
Figure 5.10 – Deep discomfort rates.	64
Figure 9.1 – Custom made GUI: components.....	83
Figure 9.2 – Stimulation trigger: start/stop sequences.	84
Figure 9.3 – Simplified scheme of separated activation of pads.	86
Figure 9.4 – Simplified scheme of asynchronous/synchronous activation.....	87
Figure 9.5 – Example of GUI running before reaching the reference value with asynchronous stimulation.....	89
Figure 9.6 – Example of GUI running right after reaching the reference value with asynchronous stimulation.....	90

List of Tables

Table 9.1 – Technical specifications of IntFES stimulator.....	81
Table 9.2 – Technical specifications of force sensor.	82

1. INTRODUCTION

1.1 BACKGROUND

Rehabilitation engineering is the application of science and technology to reduce handicaps of patients with disabilities. This is a big research area, which includes several disciplines, whose aim can be to improve from mobility, to communication abilities or sensory perception of impaired people. The main task of rehabilitation engineering is to develop technologies, techniques and methods to improve or cure impairments, but in those cases where no further improvement can be achieved, rehabilitation engineering can also provide assistive technologies that can help improving quality of life of patients [1].

Neurorehabilitation is a specific field inside rehabilitation, whose aim is to aid recovery of a nervous system injury and restore any functional alteration resulting from it. Functional Electrical Stimulation (FES) is a technique that has high acceptance in neurorehabilitation, more specifically, in restoration of motor dysfunctions caused by neurological disorders. Most applications are aimed to stroke or spinal cord injury (SCI) patients and, in short, they consist on bridging interrupted or damaged neural paths between the brain and the extremities. FES applies electrical pulses to stimulate nerve fibers and achieve a desired muscle contraction. The whole systems that allow restoring functional movements by using FES techniques are called neuroprosthesis.

In this thesis we try to contribute to this area by testing and comparing results of new stimulation methods that are now available thanks to new technologies. This study focused on upper limb stimulation with surface electrodes and analyzed different sensations perceived with application of

different methods. Results showed comfort differences between surface stimulation methods, which can be used to develop more comfortable neuroprosthesis and FES stimulation techniques.

1.2 MOTIVATION AND AIM

The main motivation to carry out these experiments was the lack of studies regarding different stimulation techniques with new multi-field electrodes. Although asynchronous stimulation has been mainly used in latest research with multi-field electrodes, synchronous stimulation is an alternative stimulation method that can be also applied with multi-field electrodes, of which no studies have been published yet.

Another reason that moved us to carry out these experiments focusing on sensation was to find if there is a stimulation method that can make surface electrode stimulation more comfortable for the users. Uncomfortable feeling perceived by receptors located in the skin can limit performance and use of FES with surface electrodes in some cases. Therefore, it is interesting to test new stimulation techniques in sensory aspects also, in order to find optimum methods that can ensure good performance producing as smallest discomfort as possible.

The goal of this study is to provide new knowledge regarding discomfort with different methods that can be used for developing more efficient and less uncomfortable neuroprosthesis.

1.3 THESIS STRUCTURE

This thesis is divided into nine chapters. Second chapter gives background information and it is divided into two subchapters. First of them describes neurophysiological basic principles and neuromuscular electrical stimulation (NMES) basis, as well as a very brief description of clinical applications of FES. Second subchapter is a review of technologies available for FES systems, which include electrodes, stimulators, neuroprosthesis and hand kinematics or dynamics analysis systems.

The third chapter presents the materials used and developed to carry out the experiments, divided into three subchapters, where each device is described in detail. Fourth chapter describes the stimulation methods that were compared in the experiments, as well as the protocol design and the procedure used for the experiments.

In the fifth chapter main results obtained in the experiments are summarized. In the sixth chapter, an explanation of results presenting differences of both stimulation methods, conclusions and possible future research are described.

Finally, chapters seven, eight and nine contain references, acronyms and appendixes respectively.

2. STATE OF THE ART

This chapter is divided into two main sections. First of them is a general and brief review of the principles of neurophysiology, so that fundamentals of FES can be understood. In addition, some clinical applications of FES are explained. In the next section, a review of actual FES devices and components is presented.

2.1 PHYSIOLOGY

The nervous system is a network of specialized tissue that controls actions and reactions in order to adjust it to the environment. All members of animal kingdom have a nervous system, but the greatest complexity is found in humans, which leads us to be vastly superior to other animals when exploiting our environment.

2.1.1 Nervous system and nerve cells

The human nervous system is divided in two main parts, which are the central nervous system (CNS) and the peripheral nervous systems. The CNS is composed by the brain and the spinal cord, while the peripheral system includes the spinal, cranial and autonomic nerves and their branches. Describing it in a simple way, we could say that the brain is responsible for processing the information and storing data, the spinal cord is the channel through which all the information flows, and the nerves act like inputs or outputs of the system, taking the information from the environment or transmitting orders to muscle or organs [2].

The nervous system has two types of cells, which are the basic units of the nervous tissue: nerve cells, also called neurons; and glial cells, which are not involved in signal processing but also have vital role like providing support to neurons among other things. In this case, we are going to focus only on nerve cells.

A neuron is an electrically excitable cell that can process, generate and transmit information through electrical or chemical signals. Information along the nervous system travels by means of electrical signals, called action potentials (AP), which are generated in the axon and are fast all-or-none electrical impulses with duration of about 1ms and amplitude of around 100mV. Every neuron has a separation of charges across its cell membrane consisting of a thin cloud of positive and negative ions spread over the inner and outer sides of the cell membrane as shown in figure 2.1. The electric current that flow into and out of the cell is carried by ions, which cause disturbances in the polarization of the membrane. A reduction of charge separation that leads to a less negative membrane potential that the one at rest, is called depolarization, and if this depolarization reaches a threshold the cell will then produce an AP [3,4].

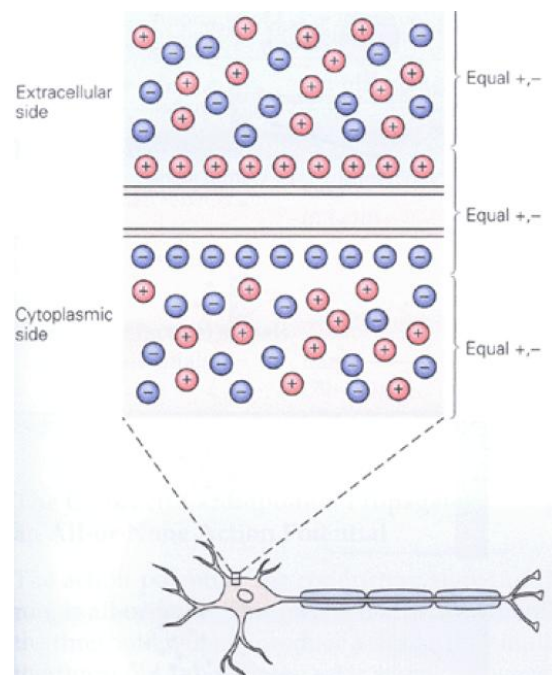


Figure 2.1 – Membrane potential on the cell membrane. Reprinted from [3].

A typical nerve cell has 4 different regions, which have different roles in the generation of signal and communication with other neurons:

- Cell body: It is the metabolic center of the cell, the nucleus.
- Dendrites: They are tree-shaped and they are the main apparatus for receiving incoming signals from other neurons.
- Axon: It is a long tubular part that extends away from the cell body and it is the main conducting unit for carrying signals.
- Presynaptic terminals: These are branches coming from the axon and are responsible for communicating with other neurons.

To increase the speed by which action potentials are conducted, large axons are wrapped in a fatty, insulating sheath of myelin, which is interrupted at regular intervals by the nodes of Ranvier. The point at which two neurons communicate is called synapse. The nerve cell transmitting a signal is called presynaptic cell and the one receiving the signal is called post-synaptic cell. All these concepts are represented in figure 2.2.

The principle of dynamic polarizations states that electrical signal flows only in one direction. In short, it begins at the input receivers, which are the dendrites and the cell body itself, which receive electrical signals from another neuron; right afterwards, the cell body sends a triggering stimulus to the axon, where an AP is generated, and finally the information reaches the synapsis, where information will be transmitted to the next neuron through the presynaptic terminals [3,4].

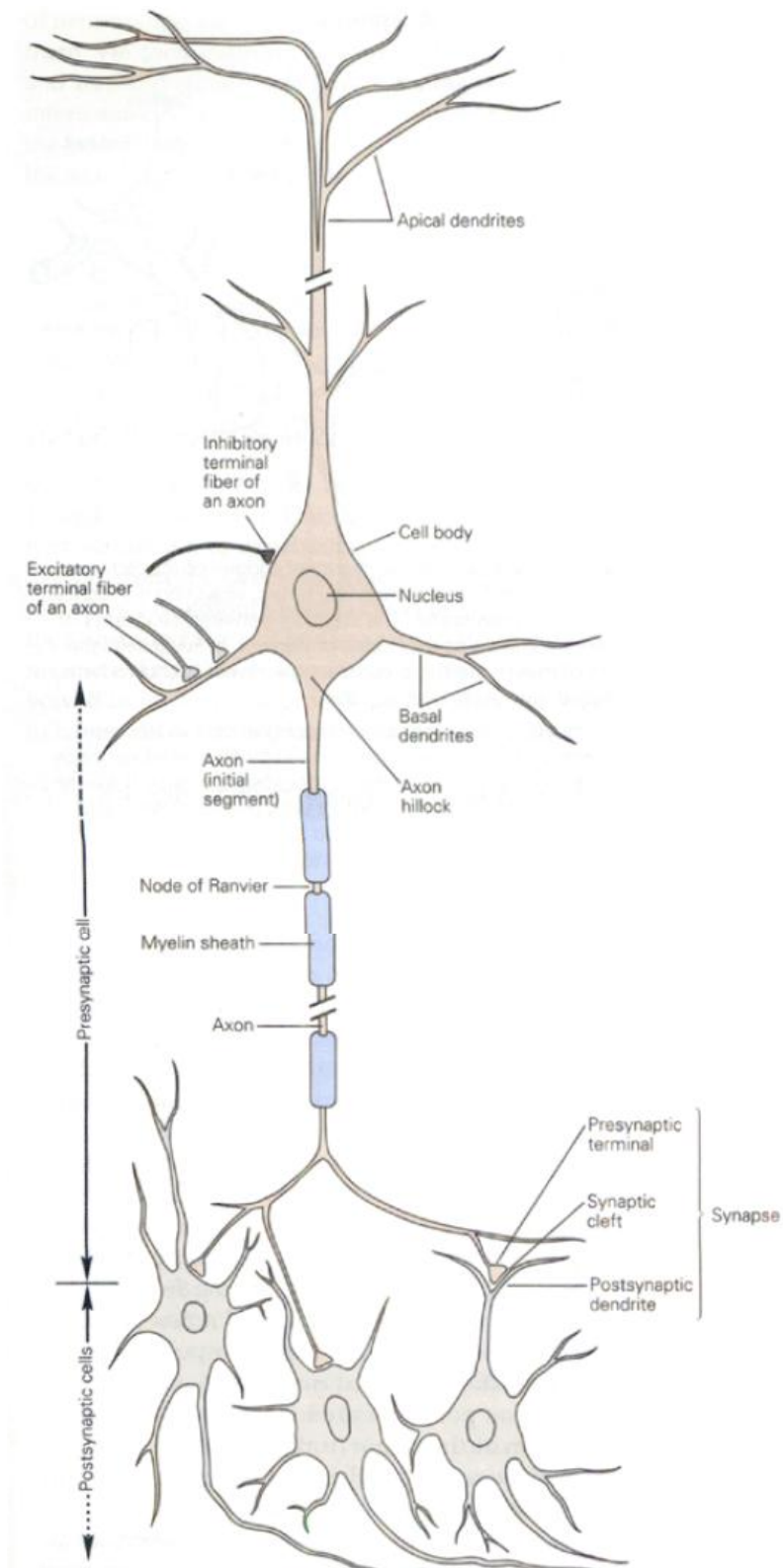


Figure 2.2 – Structure of a neuron. Reprinted from [3].

2.1.2 Movement

The nervous system is formed by a wide variety of neuron types and each of them has an important role for a proper behavior of the whole system, some examples of neuron types are shown in figure 2.3. For instance, the sensory system, which is a subsystem of the nervous system, is formed by sensory neurons, which transform physical energy from the environment into neural signals. On the other hand, the motor system produces movements by translating neural signals into contractile force in muscles. The voluntary movement is generated in the brain neurons, which send signals to the spinal cord. At this point, some signals are directly transmitted to motor neurons, although most are relayed through a variety of interneurons.

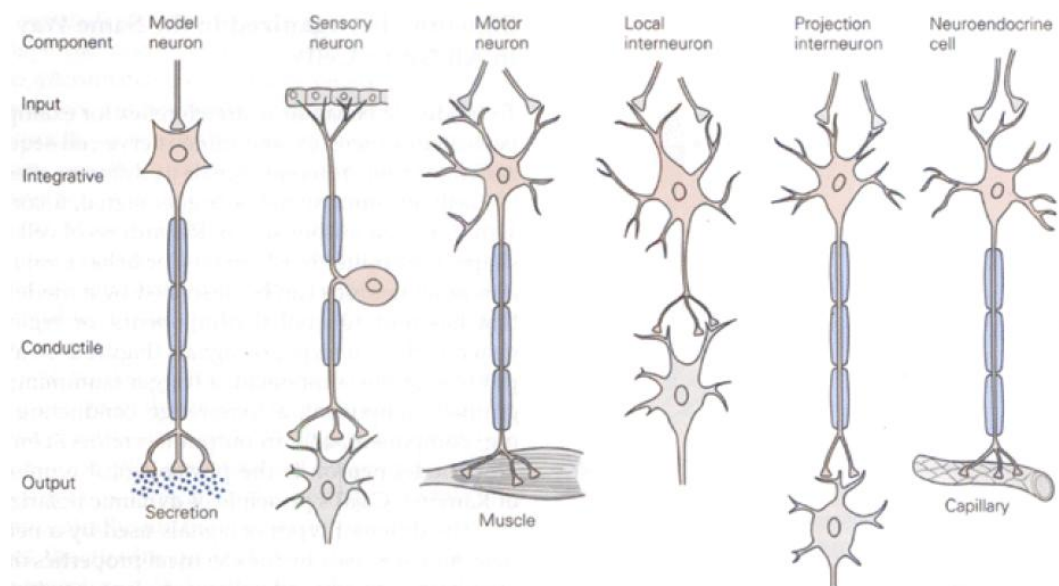


Figure 2.3 – Different neuron types. Reprinted from [3].

We are now going to focus on the musculoskeletal system, which is the mechanical apparatus by which our nervous system interacts with the outside world.

Skeletal muscle is divided into stringlike fascicles, which themselves are divided into smaller stringlike cells called muscle fibers. A typical muscle is controlled by about a hundred large motor neurons whose cell bodies lie in the

spinal cord or brain. The axon of each motor neuron exits the spinal cord through a ventral root and traverses progressively smaller branches of peripheral nerves until it enters the muscle it controls. There it branches widely to innervate anywhere from 100 to 1000 muscle fibers scattered over a substantial part of the muscle. The functional connection between a motor neuron and a target muscle fiber is a chemical synapse. The group of muscle fibers innervated by a single motor neuron is called a *muscle unit*, and this together with its motor neuron is called a *motor unit* [3,4]. An example of two motor units is shown in fig. 2.4.

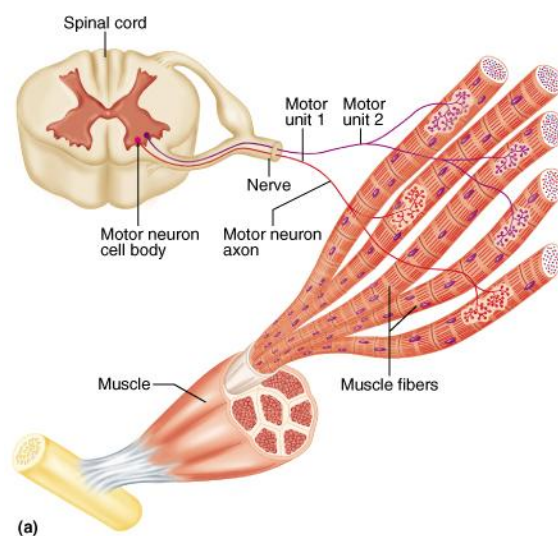


Figure 2.4 – Motor unit. Reprinted from [4].

Most muscles are composed of a mix of three fiber types: slow-twitch fibers and two types of fast-twitch fibers, where all the fibers from a motor unit are the same type.

Slow-twitch fibers, also called *type I fibers*, produce forces that rise and fall slowly in response to an AP, and muscles composed of these fibers can produce relatively small amounts of tension for long periods without fatiguing. The motor neurons that control the slow-twitch muscle fibers have smaller cell bodies and innervate fewer, thinner fibers, resulting in such small force outputs as little as 1% of the force produced by fast fatigable units.

Fast-twitch fibers, also called *type II*, produce forces that rise and fall quickly and are categorized into two subtypes. The fast fatigable fibers or type IIB fibers produce brief bursts of force, after which they take many hours to recover

fully. The fast fatigue-resistant fibers or type IIA fibers combine relatively fast twitch dynamics with enough capacity to resist fatigue for several minutes.

In both reflexive and voluntary contractions motor units are always recruited in a fixed order from weakest to strongest units. Thus when only a small amount of force is required from a muscle, force is provided exclusively by the type I fibers. As more force is required, type IIA and then type IIB units are recruited in a precise order according to the magnitude of the force each unit produces. As muscle force is decreased, motor units drop out in the order opposite from their recruitment, so the largest units are the first to cease activity.

The contractile force generated in a muscle is also dependant of its length because of the geometry of the sarcomeres. The muscle fibers are divided into even smaller stringlike cells called myofibrils, which are formed by sarcomere bands. The sarcomere is the functional unit of the muscle, which contains contractile proteins as well as thick and thin filaments as shown in figure 2.5. Cross bridges, which are the responsible for provoking a contraction in the muscle fiber, are generated between the filaments when the fiber is stimulated by an AP [3,4].

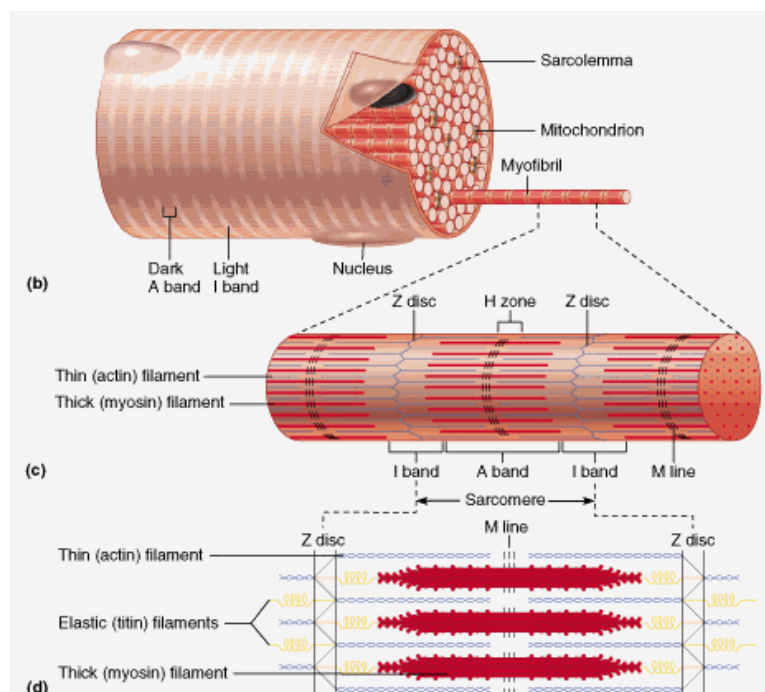


Figure 2.5 – Sarcomere structure. Reprinted from [4].

The contractile force of each muscle fiber depends on its length, so, the level of stretch or contraction of the sarcomere will condition the force that can be generated as shown in figure 2.6. The maximum force can be generated when the length of the muscle is the optimum, in its relaxed state, where the sarcomere filaments are at the optimum position. When the muscle is shortened or contracted the sarcomere thin filaments start to overlap, and force that can be generated starts decreasing. Similarly, when the muscle stretches, filaments separate, so force that can be generated also starts to decrease. But, in contrast to the previous case, when muscle is stretched contractile passive forces are generated because of mechanical properties of the muscle tissue, in particular, because of the internal resistance of the muscletendon unit to the elongation caused by the stretch [5].

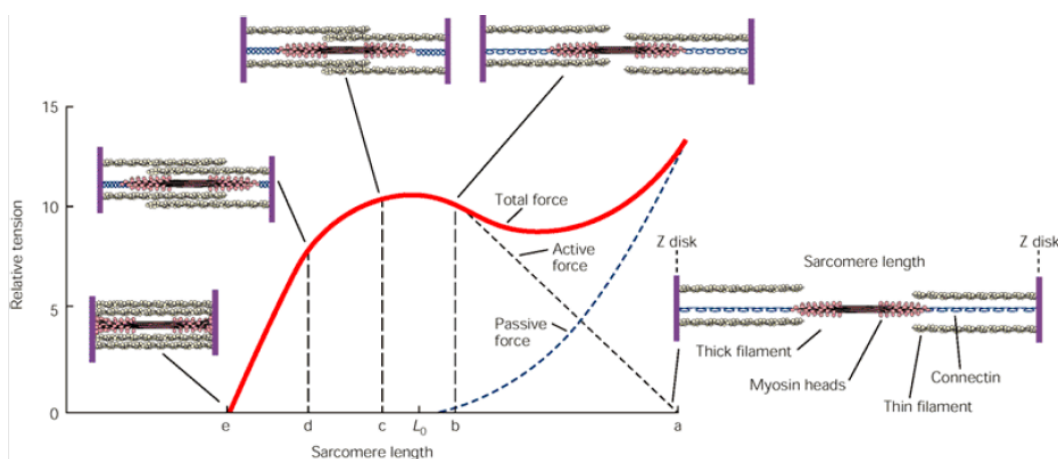


Figure 2.6 – Contractile force developed over muscle length. Reprinted from [3].

As described above, an AP is an electrical stimulus generated at the axon of a neuron and is the basic information unit of the nervous system. When an AP stimulus is received by a motoneuron a 'twitch' type myofibril contraction is produced as an output, which is all or none type and this cannot be graded by varying the intensity of the stimulus.

Alternatively, the nervous system is able to grade muscle fiber force output by modulating rates or frequency of excitatory stimulus. This is possible thanks to a process known as 'sum of contractions', which is an effect that takes place in the myofibrils. If the filaments of a sarcomere are already in a contracted

state and, before relaxing, another excitatory stimulus is received an increased force is generated. This effect is described in figure 2.7, where muscle force response to different stimulus frequencies is presented. A low firing rate will cause small tension muscle contractions, twitches in which muscle fibers are contracted and then have enough time to relax before next stimulus takes place. As stimulus are fired at higher frequencies, muscle response show higher force magnitudes and less distinction of individual twitches. Finally, if frequency of tetany is exceeded, high forces are achieved without fluctuations. Tetany is the final fusion of myofibril contractions, which result in an absence of tremor in a stimulated muscle. The tension developed by the muscle in tetanus state is usually at least four times the one evoked by individual twitches. Most of the voluntary muscle contractions are this type of contractions, smoothly fused tetanic contractions [6].

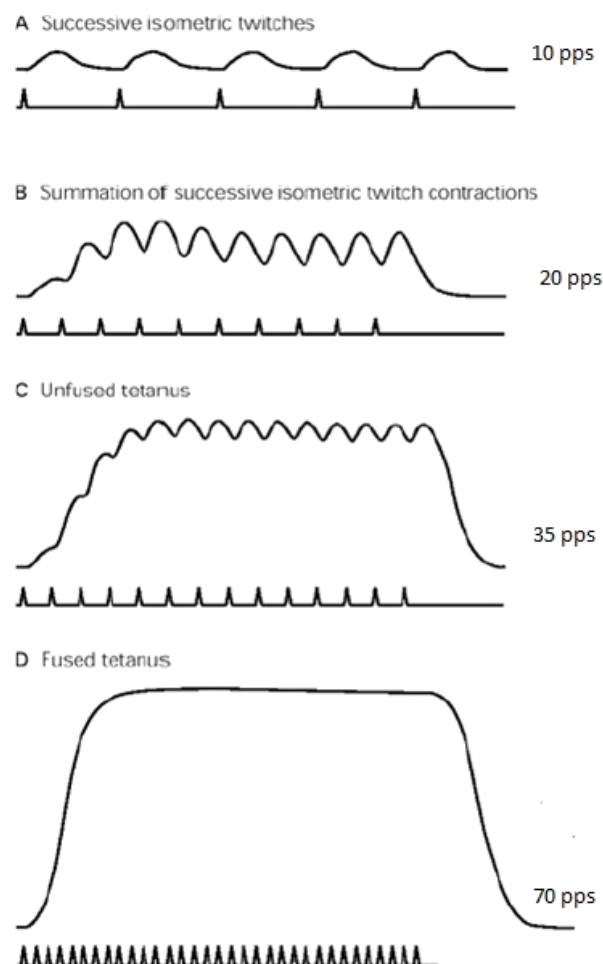


Figure 2.7 – Active tension on the muscle for different frequencies. Reprinted from [3].

Hence, natural pattern of excitation and recruitment of muscles involve combination of several parameters and asynchronous activation of different motoneurons. Different motor units are recruited asynchronously at different times and rates, with different contracting and relaxing times, and this complex system is the one that enables us to reach a vast number of smooth contractions and movements.

2.1.3 Neuromuscular electrical stimulation basis

NMES is based on the application of electric currents onto different parts of the body in order to control externally specific muscles. We will focus on the use of surface electrodes, although in next sections other approaches will be mentioned.

The basis is simple, it consists on a closed circuit where the current flows from the anode (+) to the cathode (-) passing through the nerve as shown in figure 2.8. The flow of ions moving from the positive electrode to the negative one and vice versa causes a depolarization where the current leaves the nerve membrane, usually next to the cathode. This depolarization causes an AP, which travels along the nerve until it reaches the motor neuron that will cause the correspondent movement.

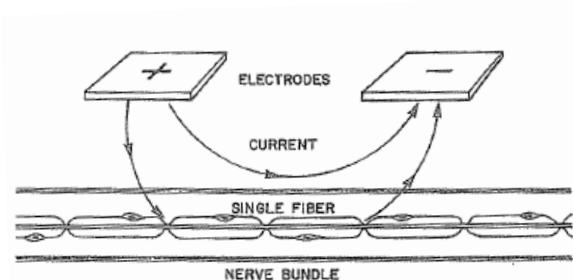


Figure 2.8 – NMES. Reprinted from [11].

Several facts affect to NMES, but first and one of the most important ones is the skin impedance, which affects significantly to the distribution of electrical fields. As Kirchoff's principle says, 'current takes the pathway of least resistance'. This means that most of the current flows through the superficial layers of the

skin, where lower impedance layers are located, bypassing the nerve as shown in figure 2.9. For this reason, larger nerve axons are more easily excited by external stimuli than small or thin nerve axons, because the bigger the section of the axon is, the lower resistance to the current it presents. Of course, physiology of each person affects enormously to the behavior of the NMES [7].

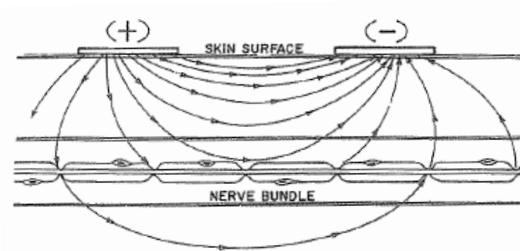


Figure 2.9 – Current distribution. Reprinted from [11].

Electrode size also affects stimulation in different ways. Current density is the amount of current flow per unit area, so low current density means a small amount of ion movement in a particular area of a tissue, which may be insufficient for depolarizing the membrane. When using same current amplitude with two different electrode sizes, the big one will have a smaller current density than the smaller one, so the smaller one should excite the membrane easier with the same current amplitude as the big electrode. Even though, there are many problems when using very small electrodes. First of all, is that the high current density in the electrode-skin interface makes it very uncomfortable due to the big amount of sensory receptors. And another problem is that a small electrode covers a very small area, which can be inefficient if it is not very close to the excitation point. Then, the solution of electrode size resides in finding the balance between performance and comfort. Usually bigger electrodes are used for bigger muscle units and smaller electrodes for smaller muscle units [8,9].

Regarding the stimulation waveform, rectangular pulses are used in a variety of configurations, although monophasic configurations are less popular because they cause electrode deterioration and skin irritation with prolonged use [10]. A scheme showing different waveforms with their advantage and disadvantages is represented in figure 2.10.

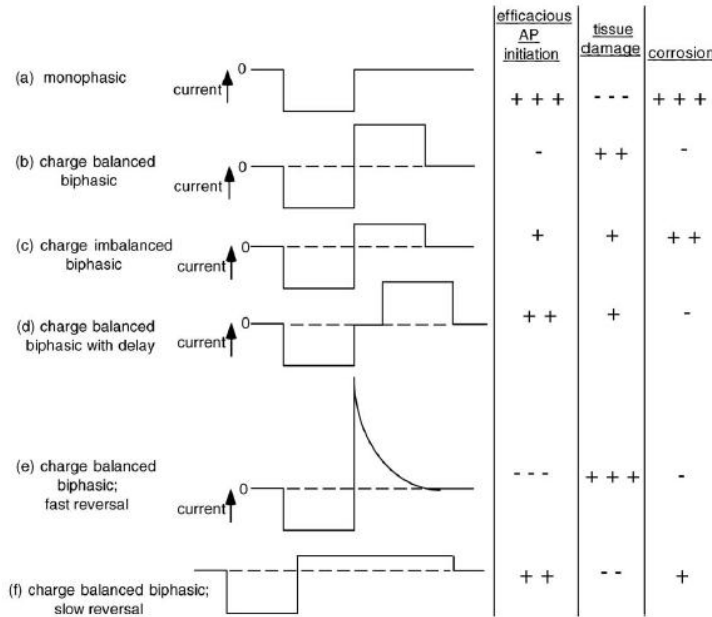


Figure 2.10 – Different pulse configurations and tissue damage. Reprinted from [10].

Stimulation parameters such as pulse amplitude, duration or frequency also affect stimulation in several ways. The amplitude or intensity of the current pulse and its duration must be adequate to successfully stimulate the muscle fibers. The fibers that are excited first are those nearest the electrode and with largest diameters. As amplitude increases smaller fibers and large fibers further from the electrode are recruited [11], as shown in figure 2.11.

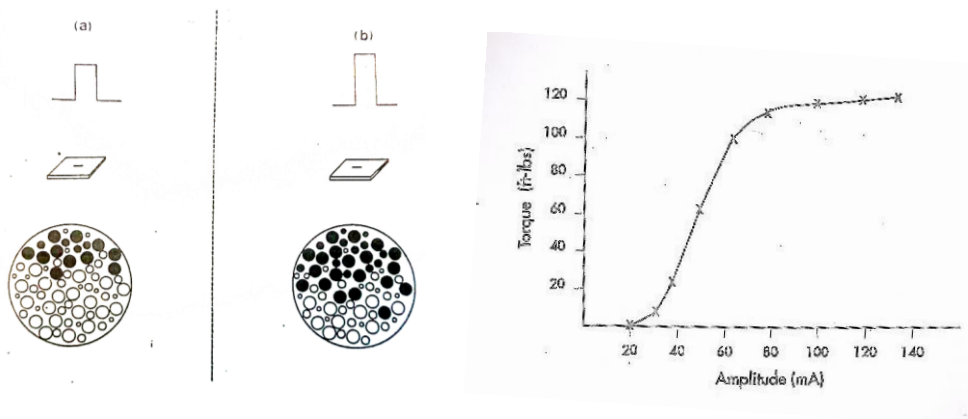


Figure 2.21 – Amplitude effects. Reprinted from [11].

Anyway, not only amplitude affects the output force, pulse duration can also contribute to this. The next curve shows the combination of amplitudes and

pulse durations needed for excitation of wrist extensors. In order to reduce amplitude and so discomfort, pulse duration is usually set between 200 μ s and 400 μ s so lower amplitudes are needed to stimulate the nerve. A graph showing combination of amplitude and pulse duration for motor threshold and maximal force generation is shown in figure 2.12.

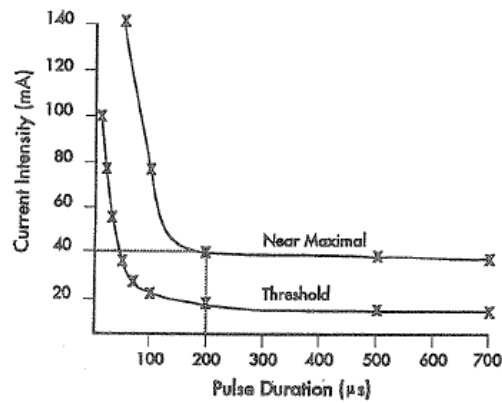


Figure 2.32 – Amplitude vs. Pulse duration. Reprinted from [11].

As explained in the previous section, stimulation frequency determines not only the produced output force, but also the type of contractions. For a tetanic contraction minimal frequencies between 25 and 50 pps are often used, but there is also another fact to take into account, because frequency affects fatigue. As shown in figure 2.13, the higher the stimulation frequency is, the faster the force decreases over time [12,13].

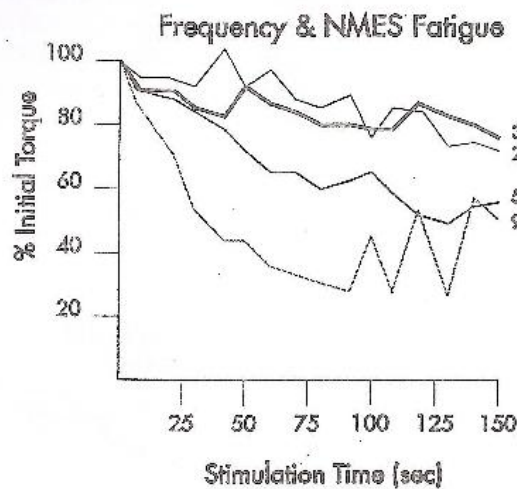


Figure 2.43 – Fatigue for different frequencies. Reprinted from [11].

Normal neural activity is asynchronous, motoneurons are excited at different times and rates and they produce smooth muscle contractions achieved with very low rates. On the contrary, by NMES, the same nerve fibers are stimulated repeatedly and synchronously with higher rates required by voluntary contractions. Indeed, fast fatigable muscle fibers are recruited first, just the opposite way to the natural recruitment order, where the small fatigue-resistant fibers are first recruited and the large fast fatigable fibers last.

In order to decrease fatigue without affecting the achieved muscle forces, different solutions have been proposed by modifying stimulation patterns on frequency and pulse width, obtaining some reductions in fatigue [14-16]. However, these methods are yet not good enough to abolish fatigue effects for long period NMES applications.

2.1.4 Clinical applications

NMES has several clinical treatment applications on neuromuscular and musculoskeletal problems. Applying external stimulation can induce therapeutic and functional motor responses for many patients who show difficulties during voluntary movement. It has been proved that NMES is successful in the following programs among other things: strengthening of muscle [17], maintenance or increase in range of motion, temporary inhibition of spasticity [18] and pain treatment [19].

Although NMES has many clinical applications, we will focus on the one regarding this project, which is the restoration of limb motor functions on patients who have damaged neural pathways. The application of NMES to substitute damaged neural motor control functions in order to achieve functional movements is called FES. Application of FES involves mainly SCI patients who still retain some sensation or movement below the level of injury, called incomplete SCI, and stroke patients. These patients' neural activity is interrupted in some sensory-motor nerve structures, which can make them unable to perform voluntary movements in some parts of their body. The consequence are paralyzed extremities or problems in motor control of upper or lower extremities (difficulties for grasping, drop foot, etc.) [20]. In this case, the aim of FES is to substitute these damaged neural pathways by applying electrical currents to the

motor nerves in order to achieve contractions in a muscle, and so, perform the desired movement. Figure 2.14 illustrates this concept.

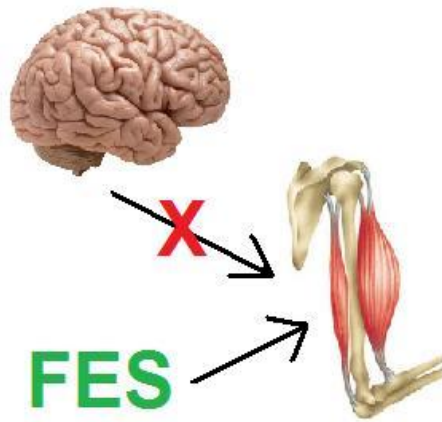


Figure 2.54 – FES to restore damaged motor function.

Regarding lower limbs, drop foot is a common gait abnormality in stroke patients that is characterized by the inability of achieving dorsiflexion of the foot. This is due to a neurological disorder caused on the brain and it is successfully compensated in some patients with stimulation of the peroneal nerve with FES, which causes ankle dorsiflexion. It has also been demonstrated that the use of FES for this purpose helps on patients' rehabilitation [21,22]. FES is also used in several applications with incomplete SCI patients in lower limbs. With patients that have good stance stability but problems with gait, FES is applied to assist the swing phase, so they can walk for short periods with help of electrical stimulation. Some others are unable to get successful sit-down to stand-up transitions, so FES is applied to assist the standing process [23-25].

Grasping impairments are also consequences of stroke or SCI, and these usually carry inability of producing voluntary wrist or finger extension, which result in big problems to achieve grasping. FES can help to restore this function as well as providing therapeutic effects [26,27]. To restore grasping, radial, median or ulnar nerves located in the forearm and shown in figure 2.15 are stimulated with one or more electrodes placed along the forearm. The radial nerve is the one responsible of provoking wrist and finger extension, whereas stimulation of median and ulnar nerves produces wrist and finger flexion [28].

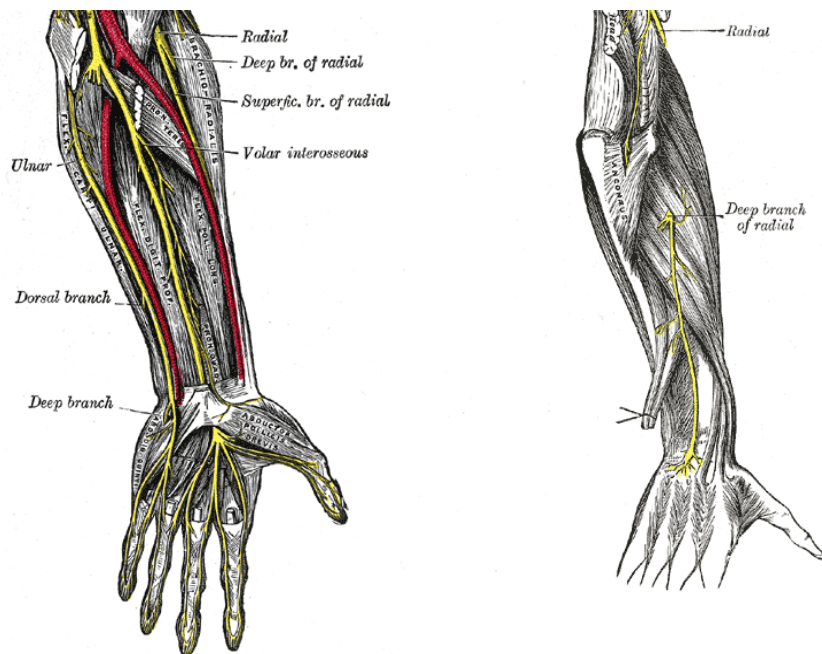


Figure 2.65 – Nerves left forearm anterior view – Nerves right forearm posterior view.

Reprinted from [28]

One big challenge is to find the adequate placement of the electrodes to achieve the desired movement, because physiological differences (muscles, nerves, fat,...) among subjects result in significant differences in optimal electrode positions. We call motor points to those points where the nerve is more superficially located and therefore, it is easier to innervate. Hence, to successfully restore grasping functions in patients, it is necessary to first find these motor points for each individual. Even if optimal points differ from individual to individual, studies have been developed to find the optimal areas where electrodes are needed to place in order to achieve grasping or releasing movements [29-31].

2.2 TECHNOLOGY

As this project is focused on upper limb stimulation, we will now describe available technology for this purpose. We will first summarize state of the art regarding functional electrical stimulation devices as well as neuroprostheses, to finish analyzing measuring systems.

2.2.1 Electrodes

Electrodes are the responsible for transmitting the electrical pulses coming from the stimulators to the motor nerves; therefore, we could say that they are the electronics-body interface, so they should be as effective and as comfortable as possible. There are three types of electrodes that we will present from the most invasive to the least.

The most invasive of all the approaches are the implanted electrodes. These electrodes are located directly onto the nerve, so open surgery is needed to place them. Usually stimulator is also implanted and placed inside the body. There are several implanted electrode types [32], we will describe some of them, which are represented in figure 2.16:

- Cuff electrode: This is a popular electrode type that it is usually attached to larger nerves; when it is closed it traps the nerve inside it. It produces reverse recruitment order, first type IIB fibers and then type I fibers.
- Wraparound electrode: This electrode is thin and flexible, which makes it more adaptable to the nerve than the cuff electrode. It is attached to the nerve wrapped around it. It also produces reverse recruitment order.
- Epymisial electrode: This electrode is often used for innervating small muscles as those located in the forearm. It is made up of a metallic disc and it is sutured to the muscle surface, usually next to the motor point.

Fully implanted grasping systems have shown successful results regarding hand function restoration but also complications like, electrode failure, need of repositioning implanted stimulator due to its rotation, typical post-surgery complications and even infection [33]. Although new methods are arising [34,35], implanted electrodes still present several disadvantages due to their invasiveness.

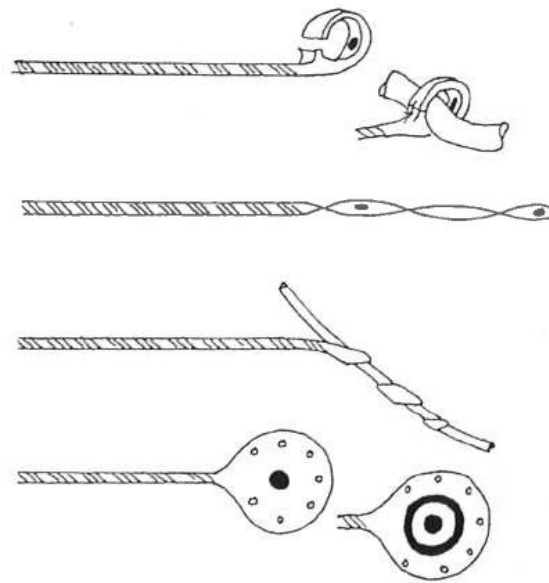


Figure 2.16 – Implanted electrode types: cuff, wraparound and epimysial. Reprinted from [32].

Percutaneous electrodes are middle way between implanted electrodes and surface electrodes. Like implanted electrodes, they are attached close to the nerve inside the skin, but unlike the previous ones, there is no need of open surgery to place them because they are placed using a hollow needle as a guide. They are provided with little barbs, which maintain them in their position. They carry some disadvantages because electronics are outside the body, meaning that users carry a bundle of wires coming out from the skin which makes this technique quite uncomfortable. Besides, electrode location is not so clear as with implanted electrodes so location very close to the desired nerve cannot be completely ensured and, as it is not attached to it, relative motion occurs when the muscle contracts. So we could say that percutaneous solutions are not so popular because it improves invasiveness level, compared to implanted electrodes, but in exchange of several disadvantages [33].

Finally, the least invasive of all the electrode types are the transcutaneous or superficial electrodes, which are not invasive and they are simply attached to the skin. For this reason, they are the most popular in FES and rehabilitation therapy applications although they carry lot of other disadvantages.

Due to the relatively high resistance of the skin, high currents are needed to stimulate nerves, which usually cause discomfort. Besides, skin and electrode resistivity are not homogeneous, which makes discomfort even worse. Electrode inhomogeneities or skin inhomogeneities due to the presence of pores, glands, structure differences or water amount differences, can cause locally high current densities and worsen stimulation comfort. Indeed, high current density at the edges of the electrode compared to the center, which is called *electrode edge effect*, is also very common in surface electrodes. To avoid these problems, high resistivity electrodes are suggested [36,37].

Still, the main problem of surface electrodes lies in the selectivity. As electrodes are attached to the skin, some deep nerves become almost inaccessible, and on the contrary, superficial nerves located next to the electrode will too easily be stimulated. As mentioned before, skin has several layers and it is inhomogeneous, which makes current distribution unpredictable. However, some models have been developed to try to predict current distribution on the skin when applying electrical stimulation with surface electrodes [37-39].

There have been several electrode types regarding material through the years. Here are listed the most popular ones [40]:

- Metal plate electrodes covered by fabric tissue: They are metal plates often covered with a spongy material that is made conductive by getting wet. An example is shown in figure 2.17. They should be fixed to the skin by means of straps. The problem is that drying of the material can cause several skin burns because of unequally distributed electrical fields under the electrode.



Figure 2.17 – Metal plate electrodes covered by fabric. Reprinted from [40].

- Carbon or rubber electrodes: These are similar to the previous ones, but metal plates are covered with carbon loaded silicone instead of fabric. An example is shown in figure 2.18. Water or gel should be placed in the side of skin contact.



Figure 2.18 – Carbon or rubber electrode. Reprinted from [40].

- Self adhesive hydrogel electrodes: They use a gel to contact a conductive member with the subject's skin. The electrode is built in a multi-layer configuration consisting of multiple layers of hydrogel. The skin interface layer includes an electrically conductive gel with relatively low peel strength for removable contact with subject's skin. A second hydrogel layer connects the substrate (a low resistive material) with the skin hydrogel layer. Between the two hydrogel layers a scrim layer can be introduced. This scrim layer is introduced to prevent slippage of the two hydrogel layers and can also serve to strengthen the multi-layer substrate. An example of the electrodes and the structure is shown in figure 2.19. Except for special applications almost exclusively self-adhesive hydrogel electrodes are used in electrical stimulation. Some studies show that hydrogel electrodes produce less uncomfortable feeling when stimulating than rubber electrodes [41].

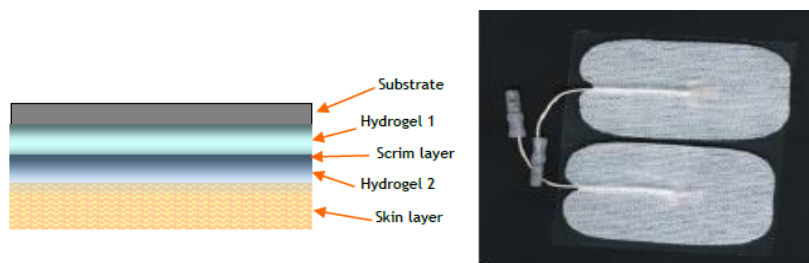


Figure 2.19 – Hydrogel electrode structure and hydrogel electrodes. Reprinted from [40].

Recently, a new electrode configuration has emerged, the multi-field electrode. An example is shown in figure 2.20. This generation of electrodes consists on a group of several tiny conductive fields, which can be activated or deactivated independently, distributed along a big area. This approach aims to improve selectivity as well as ease in don and doff of electrodes [42].

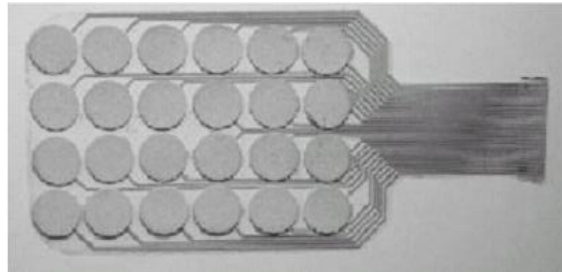


Figure 2.20 – Multi-field electrode. Reprinted from [42].

2.2.2 Stimulators

Stimulators are responsible for supplying the high current or voltages required to elicit muscular contractions, and can be configured according to the functional requirement. To provide therapeutic or orthotic support to patients, these stimulators should be safe, portable and easy to handle [43]. Some popular stimulators for surface electrical stimulation are the DUO-STIM, the Unafet 8 and the Compex Motion devices.

DUO-STIM is a medical and research device, developed in the national University of Ireland, oriented to drop-foot and blood flow augmentation applications; shown in figure 2.21. It is divided in two units, which are the programmer unit and the portable stimulator unit. The programmable unit is a user friendly programming environment for clinicians, where the algorithms for drop foot and blood flow are already implemented and clinicians only have to set stimulation parameters according to the patients. The portable stimulator unit is a wearable two-channel stimulator that provides constant-voltage biphasic stimulation. It has 4 input ports, an output voltage range from 0 to 72V, an output

frequency range from 5 to 50Hz, and an output pulse width range from 100us to 500us [44].



Figure 2.21 – DUO-Stim stimulator device, programmer and portable stimulator units.
Reprinted from [43].

Another stimulator is the UNAFET 8, which was built by UNA Systems in Belgrade; shown in figure 2.22. This device does not have any specific application program integrated; it simply allows easily setting several stimulation parameters through the screen for different purposes or applications. It is an eight-channel stimulator that provides constant-current monophasic stimulation. It has an output current range from 0 to 50mA, an output frequency range from 5 to 80Hz, and an output pulse width range from 0us to 1000us [45].



Figure 2.22 – UNAFET 8 stimulator. Reprinted from [45].

Finally, the Complex Motion stimulator, developed in Zurich presents one of the most versatile and flexible commercial systems for surface FES. It is shown in figure 2.23. It was designed to be used as a medical device for any FES application therapy, as a neuroprosthesis or as a research tool. It is a four channel stimulator that provides constant-current biphasic or monophasic

stimulation. It has 3 inputs, although one of them is for special purposes; an output current range from 0 to 120mA, an output frequency range from 1 to 100Hz, and an output pulse width range from 0s to 16ms. Apart from the stimulator, it includes graphical user interface software that is installed in the personal computer (PC) and allows building custom-made programs for a wide range of surface FES applications. It also includes chip cards where custom-built programs can be stored [46].



Figure 2.23 – Compex Motion Stimulator. Reprinted from [46].

2.2.3 Upper-limb transcutaneous neuroprosthesis

Wearable FES devices whose aim is to restore damaged sensory or motor functions are called neuroprosthesis. There are many types of neuroprosthesis, from implanted devices like pacemakers to transcutaneous devices like drop foot correction systems, but in this section we will focus on upper-limb surface neuroprosthesis. Although many custom-made grasping neuroprosthesis have been developed for research, some of the most popular devices will be mentioned.

- NESS H200 Wireless

It is the last version of a hybrid orthopedic-neuroprosthesis device developed in Israel and distributed by Bioness Inc. The system is shown in figure 2.24 and it is used to generate grasping function in tetraplegic and stroke subjects. The concept is simple, it only has 3 channels that stimulate the finger flexors, finger and wrist

extensors and thumb flexion. These 3 electrodes are controlled with a push button that triggers hand opening and closing functions. Therapists design the proper stimulation program for each patient and then the patient can bring it home and use it without any assistance. The device is composed by two parts: the hard plastic orthosis and the wireless control unit, which is a hand-held remote control box that allows users to adjust stimulation level and turning on and off [47].

One of the disadvantages of the NESS H200 is that it does not provide the possibility of adjusting electrode position because they are fixed to the orthosis. In addition, the stiffness of the orthosis does not permit supination when users wear the device.

Despite this, it is very easy to don and doff, it is exceptionally well designed, and it is in a very advanced design stage, what makes it one of the best grasping neuroprosthesis available in the market [48].



Figure 2.24 – NESS H200 Wireless: 1-orthosis, 2-control box. Reprinted from [47].

- ETHZ – ParaCare

This neuroprosthesis was developed in Zurich and it was designed to improve grasping and walking functions in SCI and stroke patients. It is based on the use of the Compex Motion stimulator, which allows a wide variety of custom made programs and integration of any sensor or sensory systems. Based on this, the

ParaCare system can be controlled with proportional electromyography (EMG), discrete EMG, push button and sliding resistor strategies [49]. Although the system permits great flexibility for a broad number of applications, donning and doffing the device is complicated and takes time due to the need of individually placing all the electrodes in the correct positions. The device is not commercially available.

- Bionic Glove

This neuroprosthesis was developed in Canada and it was designed for SCI patients who have voluntary control over wrist flexion and extension but cannot grasp successfully. The neuroprosthesis consists on a neoprene fingerless glove provided with a sensor (inductive linear variable displacement transducer) on the palm to detect wrist position. Three surface electrodes are used to stimulate finger flexion or extension following a simple strategy: when the patient flexes the wrist, the finger extensors are stimulated causing hand opening. On the contrary, when the patient voluntarily extends the wrist the finger flexors are stimulated to provide hand closure. A dead-zone allows movement of the wrist once the “open” or “close” stimulation pattern is activated. The stimulator is integrated in the glove, in the dorsal forearm part, and it has a user friendly interface with three buttons to set the stimulation parameters [50]. Some studies show successful results with tetraplegic patients but disadvantages like difficult donning and doffing and improvable control have been pointed out [51]. This device is not commercially available.

2.2.4 Hand kinematic and dynamic analysis systems

There are several research areas around hand kinematics and dynamics analysis; different approaches like visual hand tracking systems, instrumented gloves or wrist and finger force measurement systems can be used for several

applications like virtual reality, computer human interaction, hand functional assessment,...

FES-hand models:

Before describing different methods of acquiring data it should be mentioned that several models try to describe the behavior of different joints and muscles as a result of applying FES. Many solutions have been proposed through the years for many different applications and using different methods [52-58]. However, all these share a big disadvantage, which is the big complexity of the models. Most of them require a huge amount of physiological parameters which are very difficult or impossible to get in vivo. Approximated values are suggested, but this can affect accuracy of results. Besides, most accurate models are usually designed for very specific cases. Some other models follow another approach which is simplifying as much as possible the model at cost of getting approximated results [59]. Thus, lack of accurate general models for several applications, their complexity and the difficulty of defining a big amount of parameters, does not make musculoskeletal models a popular method for designing or evaluating neuroprostheses.

Computer vision based methods:

There are several computer vision-based techniques for hand gesture recognition, hand pose estimation or hand tracking, so we will just mention some examples. One of the methods is the bare hand tracking, which is still an active area of research, and most solutions consist of detecting edges and silhouettes of the hand [60-62]. These solutions are usually very robust, but their disadvantage is that they are computationally expensive algorithms, although some simpler algorithms are also proposed at cost of robustness and resolution [63,64]. Another vision-based solution consists on data-driven pose estimation. This technique consists in estimation of hand gesture based on databases that contain several possible hand gestures. An example of a gesture database and matching is shown in figure 2.25. In some approaches, fast, approximate nearest-neighbour techniques allow fast gesture recognition [65,66].

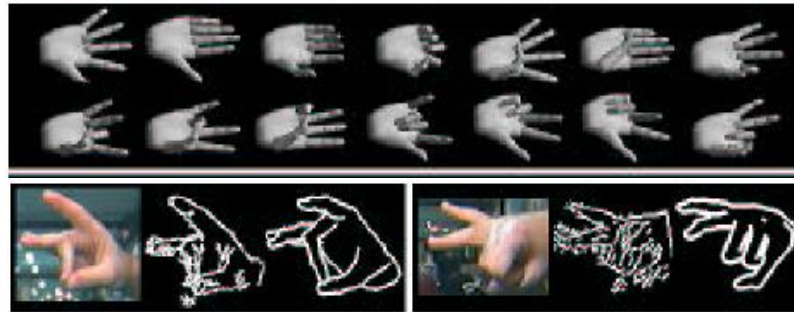


Figure 2.25 – Data driven pose estimation method: Pose database and matching.

Reprinted from [66]

There are many other vision-based techniques for hand gesture recognition, for example, a color glove approach, which is a combination of color tracking and data-driven pose estimation [67]. Considerable research efforts and methods have been developed in many research groups around the globe, which are analyzed in published reviews [68]. Main disadvantages regarding computer vision approach for hand kinematics analysis are the next [69]:

- High-dimensional problem: the hand is an articulated object with more than 20 degrees of freedom (DOF) which makes the models extremely complex.

- Self-occlusion: the hand is articulated with many-self occlusions, which is difficult to manage because some parts of the hand become hidden under other parts of the hand.

- Processing speed: computer vision systems need to process huge amounts of data, which makes it difficult to develop accurate real-time solutions.

- Uncontrolled environments: lightning changes or even objects located in an arbitrary place on the background can affect the performance of the system, which restricts its use in different environments.

- Rapid hand motion: the hand has very fast motion capabilities, compared to off-the-shelf cameras, which usually support up to 30–60 Hz frame rates. The combination of high speed hand motion and low sample rates adds complexity to the hand tracking algorithms.

Instrumented gloves:

Another approach for hand movement data acquisition are the instrumented gloves, which consist on gloves provided with different sensors located along the fingers or on the palm to measure different hand positions, hand kinematics, finger flexion, etc.

The development of glove-based systems started about 30 years ago and still it is a very active research area, so several methods have been proposed by many research groups, and although not all of them are commercially available, the instrumented glove market is actually growing.

First glove prototype was the Sayre Glove, which was developed in the 70s and was based in sources of light and photocells to measure finger bending level. Another early prototype was the Digital Entry Data Glove, which was provided with different type of sensors: touch or proximity sensors, bend sensors, tilt sensors and inertial sensors. These solutions had limited functionality and were hard-wired so they were never commercialized [69]. First instrumented glove on the market was the Data Glove, which was commercialized in 1987 and was provided with flex sensors [69]. From then on, several alternatives have arisen on the instrumented glove market for a wide range of applications. Some of the most popular are the next:

- CyberGlove: developed at Stanford University and distributed by CyberGlove Systems, it has 18 or 22 piezo-resistive sensors to measure bending of each joint of the fingers and wrist. It is shown in figure 2.26. Some versions also include vibro-tactile feedback sensors [70,71].



Figure 2.26 – Cyberglove. Reprinted from [70].

- Humanglove: distributed by Humanware in Italy, it is equipped with 22 Hall-effect sensors that measure flexion, extension, abduction and adduction of each

finger and the thumb and flexion and abduction/adduction of the wrist [72]. It is shown in figure 2.27. Modifications based on Humanglove have also been proposed for medical assessment applications [73].



Figure 2.27 – Humanglove. Reprinted from [72].

- 5DT Data Glove: commercialized by Fifth Dimension Technologies, it uses proprietary optical-fiber flexor sensors, with a light-emitting diode (LED) and phototransistor placed in each finger, so the finger bending is measured indirectly based on the intensity of the returned light. It is shown in figure 2.28. It can measure finger and thumb flexion and finger abduction and adduction [74].



Figure 2.28 – 5DT Data Glove. Reprinted from [74].

- Pinch Glove: it was developed in the University of Central Florida and it is commercialized by Fakespace Laboratories. It uses electrical contacts at the fingertips, on the back of fingers, or in the palm. When two or more electrical contacts meet, a conductive path is completed and a posture can be made. The PinchGlove provides an interface to detect postures, which makes the PinchGlove excellent for posture recognition [75,76].

- DGTech VHand: it is distributed by DGTech Engineering Solutions and consists of five bending sensors that measure finger flexion and an accelerometer located on the palm to measure wrist acceleration and orientation (roll and pitch) [77]. It is shown in figure 2.29.



Figure 2.29 – DGTech VHand with reference axes. Reprinted from [77].

- Stringlove: it is a Japanese solution distributed by Teiken Limited. It uses 24 inductocoders to record angles of fingers and thumb, abduction/adduction angles of fingers and thumb, as well as wrist motion. It is a washable glove and sensors are easily detached [78,79].

Force measurement systems:

The systems we have described so far are able to analyze hand motion, but in most FES applications it is also interesting to analyze hand dynamics and analyze forces and torques generated by fingers or wrist.

Although there are many solutions proposed in hand motion analysis, it is more difficult to achieve a low cost, wearable, light and reliable force measuring system, which has resulted mainly in isolated and custom-made hand force measuring systems for determined applications. In FES applications where specific torque measurements are needed, usually isometric approach is preferred to non isometric one because it carries a simpler procedure. Isometric forces are those where the muscle contracts and produces torque but it does not change its length and therefore neither changes the joint angle. We can say that isometric muscle contractions are carried out in fixed positions, an example could be pulling a heavy object without moving it. On the contrary, non-isometric contractions are those in which the muscle contracts and as a result muscle

length changes and a movement is generated, so it is a contraction carried out within a range of motion. Included in this last group, we find the isokinetic contractions, which are those contractions that produce a movement with a constant speed [5].

Developing a custom-built isometric force dynamometer is relatively easy, usually these setups consist on a force transducer or strain gauge attached to the stimulated limb, preventing it from moving. However, some more sophisticated setups have been developed mostly for the upper limb to satisfy the needs of measuring both wrist and finger forces [80,81]. For isokinetic force measurements of the wrist and fingers, less has been developed. One of the first commercial available dynamometers that allowed both static and dynamic measurements of wrist forces was called Cybex II, which was developed in the 80s, and it showed reliable results [82]. A modern example of a complete dynamometer allowing force measurement of isokinetic and isometric contractions both in upper and lower limbs is the S4 from Biodex Systems. This system, which is shown in figure 2.30, can be used for a wide variety of testing, training or treatment applications like sports and orthopedic medicine, pediatric medicine, neurorehabilitation, older adult medicine, industrial medicine, research, etc. [83,84].



Figure 2.30 – Biodex S4 dynamometer. Reprinted from [83].

However, lack of simple and economical solutions prevent expanding these complex dynamometers to therapeutic applications. Grip dynamometers for measuring isometric grasping force and hand-held dynamometers for measuring isometric wrist forces are economical and simple alternatives to previously mentioned complex systems for therapeutic hand force assessment applications.

Their reliability is similar to other sophisticated systems, which together with the ease of use, makes them very popular among therapists [85, 86]. There are several hand dynamometers in the market, figure 2.31 shows some examples.



Figure 2.31 – Example of hand-held dynamometer and grip dynamometer. Reprinted from [87].

3. MATERIALS

3.1 INTFES STIMULATION DEVICE

The FES device that we use in these experiments is the IntFES stimulator device, shown in figure 3.1, which was designed for functional electrical therapy (FET). It is a single channel electronic stimulator that provides constant-current biphasic stimulation. It has 6 inputs, an output current range from 0 to 50 mA, an output frequency range from 1 to 50Hz, and an output pulse width range from 50 to 1000us. It is fully controlled remotely via Bluetooth and apart from the stimulator, it includes graphical user interface software that is installed in the PC and allows setting stimulation parameters.



Figure 3.1 – IntFES stimulator.

Although it only has one channel, the IntFES stimulator was designed to control and energize up to 16 fields or pads of two IntFES electrodes. The IntFES electrodes are multi-field electrodes, also called array electrodes, which are electrodes that are divided into a certain number of fields that can be activated

independently and with different current amplitudes. Some examples are shown in figure 3.2. This configuration allows an easier donning and doffing than with single electrodes, because instead of attaching and detaching the single electrode until finding the motor point, IntFES electrodes allow attaching the electrode once and then find the motor point only activating and deactivating the different fields. Besides, depending on the configuration, shape and size of electrodes; same electrode can be big enough to cover different motor points that produce different movements and then we are able to make combinations of these. The electrodes are custom-designed, what means that can be any size or shape.

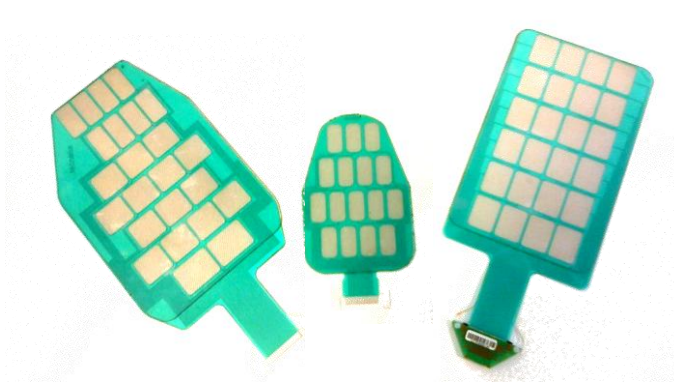


Figure 3.2 – Different IntFES array configurations.

For our experiments we used an only 16 field electrode matrix specially designed for the dorsal forearm stimulation; shown in figure 3.3. The hydrogel was high impedance hydrogel in order to reduce current distribution inhomogeneities and improve comfort [36]. The hydrogel we used was AG803 from AmGel Technologies, which has a volume resistivity of 15000 ohm-cm minimum and 30000 ohm-cm maximum [88].

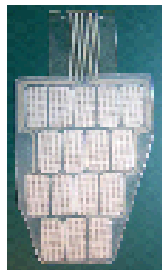


Figure 3.3 – Electrode designed for forearm stimulation.

The IntFES device has one last element, the IntFES electronic board, shown in figure 3.4, which is the interface between the stimulators and the electrodes. This electronic board is provided with a microcontroller and a multiplexer among other things, which will process the information coming from the stimulator and then will determine the activation of the pads. The IntFES electronic board is connected to the electrodes and the stimulator. This last connection is carried out by means of a thin and flexible cable and an easy to attach and detach push-pull connector, where communication protocol is Inter-Integrated Circuit (I2C) [89,90].



Figure 3.4 – IntFES electronic board and connector of the stimulator cable.

3.2 WRIST TORQUE MEASURING SET-UP

Measuring performance of FES effects on the upper limb can be done in several ways and different approaches. In the previous section we described some of the common solutions for acquiring data from hand kinematics and dynamics. A simple torque measuring solution was preferred for two reasons.

First of them was that the aim of the experiment was to compare performance between two methods easily, and due to the difficulty of achieving same movements with FES in every subject, the experiment would be based in simple movements of the wrist, without need of paying attention to finger motion or finger torque.

Second reason has to do with wrist joint stiffness. As we explained before, activated muscles create forces that are a combination of two types of tension, active and passive tensions. Active tension refers to the forces created in the sarcomeres, passive forces, instead, refer to the internal resistance of the muscletendon unit to the elongation of the stretch [5]. This internal resistance to

stretching of muscles, also called stiffness, affects range of motion of the joints and differs from individual to individual. For instance, achieving a certain extension on the wrist can suppose a big effort or a need of big torques in the wrist due to the stiffness in the flexor muscles for a subject; on the contrary, for another subject with higher flexibility level on the flexor muscles can suppose a very small effort to achieve same extension of the wrist as the previous subject. Thus, achieved movement can be completely different in two subjects even if the same torque is being generated in the wrist. Moreover, differences in size and weight of hands of different individuals also result in different resistance levels to joint motion [5]. So, for these reasons, we decided to go for a dynamic approach measuring wrist torque, which permits comparing performance between methods and among individuals easier and in a more reliable way than with other approaches.

For these experiments a purpose-built wrist torque measuring set-up was designed and built. The set up was based on a JR3 force sensor 45E15A-I63-AF, with a load rating of 1000N and 6 DOF, which provides force and torque measurements on three axes (X,Y,Z). Orientation of these axes is shown in figure 3.5. The JR3 force sensor is a monolithic aluminum device containing foil strain gages, which sense the loads imposed on the sensor. The strain gage signals are amplified and combined to become analog representations of the force loads on the three axes and the moments or torques about the three axes. The X and Y axes are in the plane of the sensor body, and the Z axis perpendicular to the X and Y axes. The reference point for all loading data is the geometric center of the sensor [91].

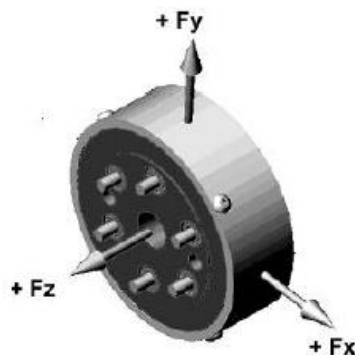


Figure 3.5 – Force sensor and orientation of three axes (X,Y,Z).

As the purpose of the set-up was to measure wrist torque, our solution consists in an aluminium structure where the force sensor is integrated as shown in figures 3.6 and 3.7. The force sensor is mounted screwed between two aluminium plates that are supported at a certain height from the base. The aluminium plate on the front has holes distributed along a circumference of 10 cm with a separation of 10 degrees between them that go from -50 to 90 degrees. The aim of these holes is to hold a bar that fixes the position where the isometric torque measurement will be carried out. On top of this bar, which can be located in any of the holes of the aluminium plate, a plastic plate is supported, which is used to support the hand. Thus, when the wrist produces a torque, forces will be transmitted to the plastic plate, which will transmit them to the bar where it is supported. This bar will be fixed in any of the holes of the aluminium plate, so it will transmit these forces to the aluminium plate, and finally, to the force sensor. The force sensor produces analog output, which is collected by a National Instrument NI-USB 6218 Data Acquisition Card (DAQ Card) and connected via Universal Serial Bus (USB) to the PC. Torque measured in Z edge will be directly the torque generated on the wrist on an isometric contraction in a determined position. Because of this, it is very important to ensure that the wrist is well aligned with the Z axis, so, the structure parts that support the forearm and hand can be adapted to different hand and arm sizes by easily changing some components to achieve this alignment.

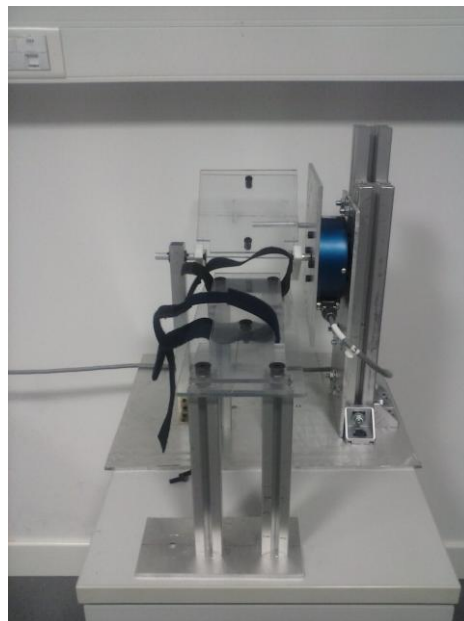


Figure 3.6 – Frontal view of wrist torque measuring set up.

The hand is facing down fixed to the plastic plate with an additional Velcro strap, so this way torque in both directions can be measured. If the bar is located underneath the plastic plate, the torque measured in the force sensor will correspond to the sum of both torque generated by gravity forces and torque generated in the wrist by flexor muscles (torques in same direction). If the bar is located on top of the plate, the value of the force sensor will represent the sum of both the torque generated on the wrist by muscle extensors and torque generated by gravity forces (torques in opposite direction).

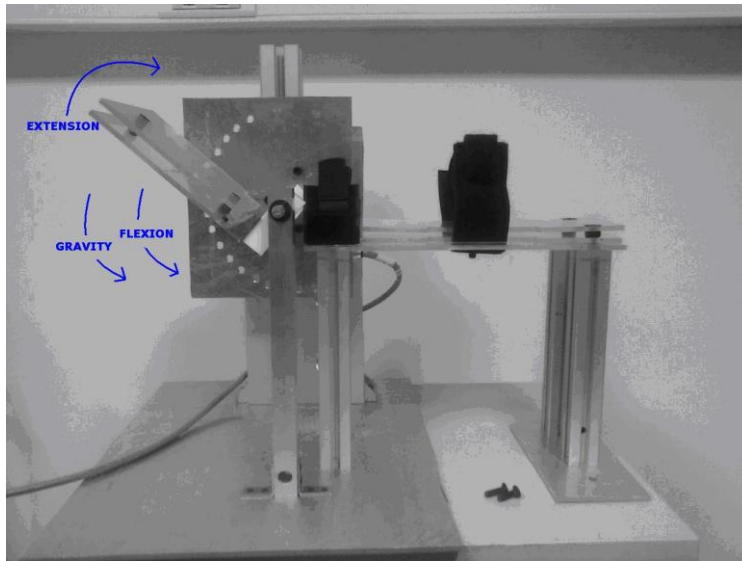


Figure 3.7 – Lateral view of wrist torque measuring set up.

To validate the whole set-up, error estimation and gage repeatability and reproducibility (Gage R&R) studies were carried out [92].

First, torque produced around the Z axis due to a 256 gr. weight located on the plastic plate was measured. Static measurements were done for the full range, from -50 to 90 degrees, 13 times. The weight for the calibration tests was chosen on purpose to produce smaller torques than posterior experiments with FES, to make sure that measured data would be reliable. First, theoretical torque generated in each position was calculated and then, it was compared to obtained measurements. Figure 3.8 shows the theoretical torque generated by a 256 gr weight in each of the positions (pink line) and real measurements of the 256gr weight in each of the positions (rest of lines).

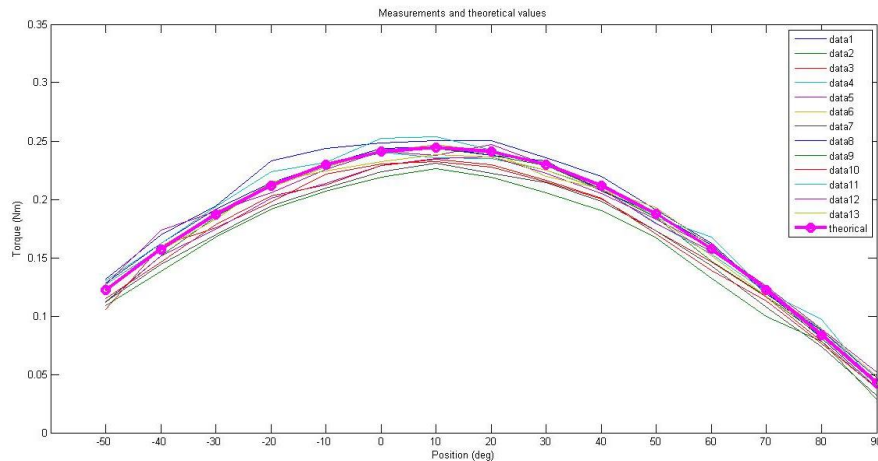


Figure 3.8 – Theoretical values compared to measurements.

With this data, the mean square error (MSE) was calculated for each of the positions and a maximum error of 0.0001 was achieved in -20 degrees position as shown in figure 3.9.

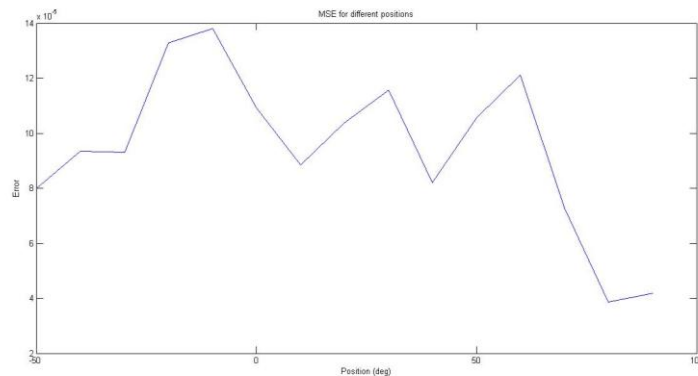


Figure 3.9 – MSE values for each position.

Then a Gage R&R based on ANOVA analysis was applied to the data. These tests were done by an only operator, which was the same that would carry out all the experiments, so the analysis results showed only repeatability results and not reproducibility results. Data was analyzed with Minitab statistical software [93] and the obtained results are shown in figure 3.10.

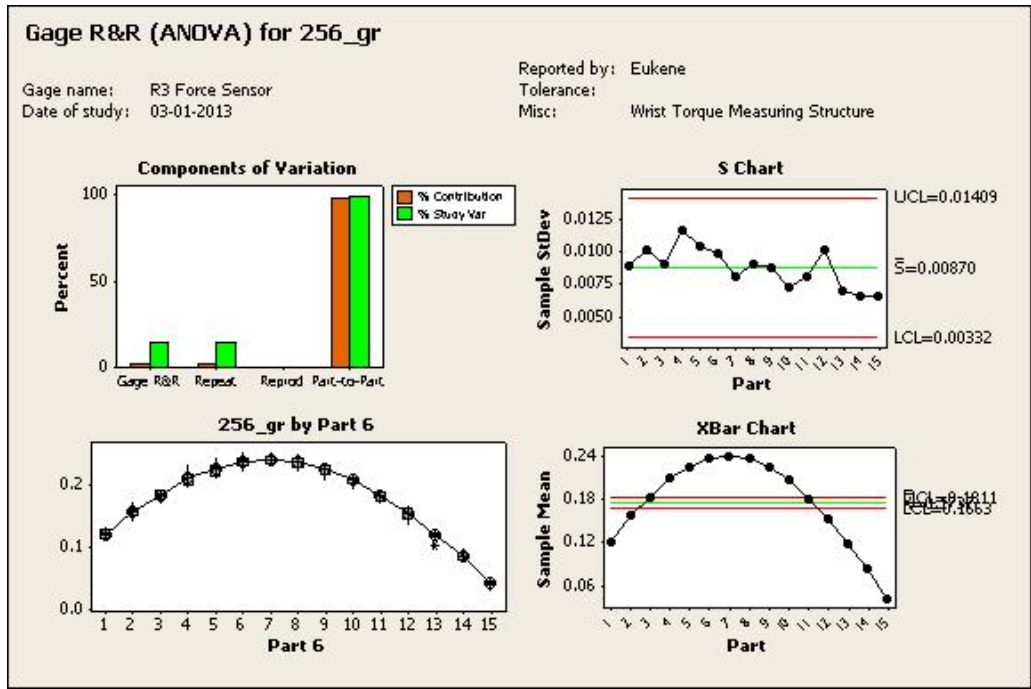


Figure 3.10 – Gage R&R repeatability results.

The results proved that the set-up could successfully differentiate slight torque differences caused by position changes. First graph in figure 3.10 shows that the variability in measurements across different positions is much bigger (98,97%) than variability caused by repeatability issues (14,34%). Second graph shows that deviations in all positions are within the control limits and the average standard deviation for all data is 0.0087. Third graph from figure 3.10 shows all the measurements with data distributed in boxplots for different positions and mean values for each position. Finally, fourth graph presents measurements and control limits, where it is shown that variations between means in different positions are higher than tolerance limits.

Summing up, the results showed that the reliability of the force-sensor together with the structure was good enough to carry next experiments.

3.3 USER INTERFACE (MATLAB)

As we described in the first section of this chapter, the IntFES stimulator is fully controlled remotely by a PC with Bluetooth communication. Although it comes with software that consists on a graphical user interface (GUI) to change stimulation parameters, it has limited functionality, so we decided to design and develop a specific purpose-built GUI for these experiments, which is shown in figure 3.11. A brief description of the GUI is done in this section and a more detailed explanation is given in the appendix.

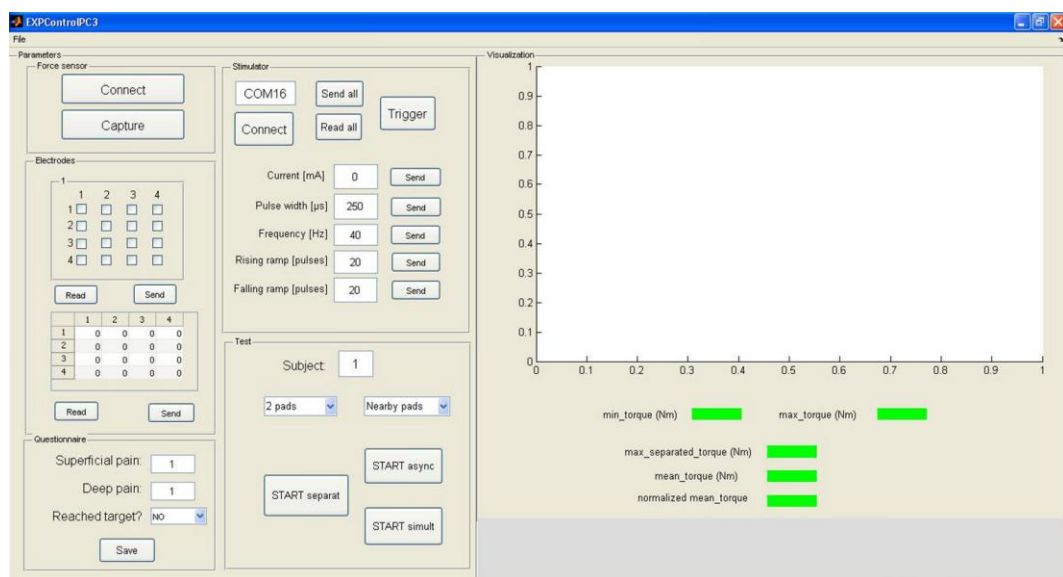


Figure 3.11 – Custom made GUI (different parts marked).

The GUI was developed on Matlab software, and its aim was to integrate the force sensor information, its processing, and the stimulator control in the same software, being adapted to these specific tests in order to simplify and shorten the experiment procedure. Matlab has an interactive environment that provides tools for designing and programming GUIs, which is called Graphical User Interface Development Environment (GUIDE). With this tool the appearance and design of the GUI is defined graphically, so then only the callbacks must be coded, which are the routines that are executed when the user interacts with the GUI. Summing up, GUIDE allows us programming the functional code and forgetting about programming the design part, which is intuitively done with this environment [94].

The GUI was separated in various sections in order to have information and tools grouped together according to their functionality, and hence, make the GUI more user-friendly. Different components of these sections provide us with different functionalities to control and supervise different parts and stages of the experiments, which are the following:

- Establish connection between PC and force sensor and stimulator
- Collect data from force sensor
- Configure stimulation parameters
- Send commands to stimulator
- Select test parameters
- Start and stop separated, asynchronous or synchronous test procedures (described in next chapter)
- Enter and save pain rates
- Display messages coming from stimulator, visualize data from force sensor in graphs and display processed force sensor data values.

Structure and functionality of the GUI is explained in more detail in the appendix.

4. EXPERIMENTS

4.1 STIMULATION METHODS

Recently suggested multi-field or matrix electrodes bring multiple new possibilities to FES. They lead to new stimulation methods that need to be tested and in this study we will try to see the differences between two of them, which are asynchronous stimulation and synchronous stimulation.

4.1.1 Asynchronous stimulation

Asynchronous activation allows us to activate different electrode fields one right after the other with 2 ms between pulses as shown in figure 4.1. Some research suggests that superposition principle is applicable to asynchronous stimulation as far as time between pulses of different fields is small enough [26]. This means that asynchronous activation of multiple fields would produce a movement equal to the sum of the movements produced by each single field.

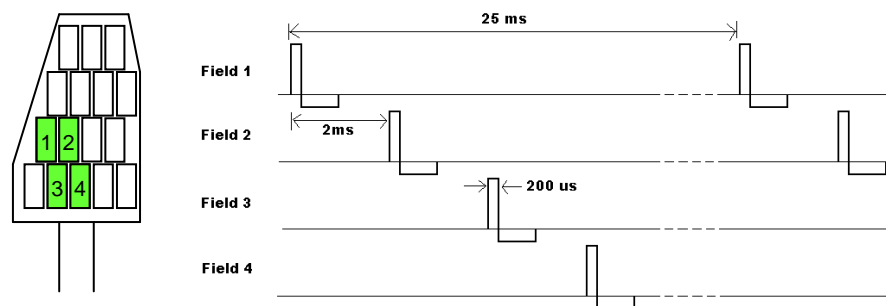


Figure 4.1 – Asynchronous stimulation.

4.1.2 Synchronous stimulation

Synchronous stimulation consists on a simultaneous activation of fields as shown in figure 4.2. In this approach current is distributed among all the activated fields at the same time; hence, fields activated synchronously would act like a single big electrode as far as the matrix used a proper gel and had proper gap sizes among fields [37].

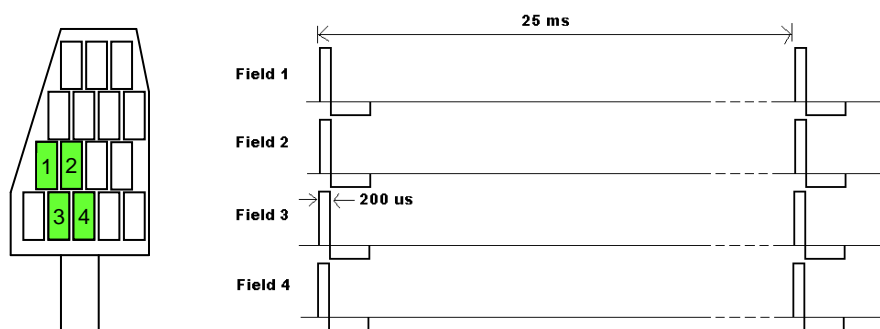


Figure 4.2 – Synchronous stimulation.

4.2 PROTOCOL DESIGN

The aim of the experiments was to see if any difference in sensation or performance could be clearly perceived between asynchronous and synchronous stimulation in a population of 15 healthy subjects.

For this purpose, we had to define an easy way of comparing FES results among individuals, so we decided to go for an isometric wrist extension torque measuring approach, due to the possibility of easily producing wrist extension with FES in every subject compared to specific finger extensions. However, the isometric approach does not allow seeing differences in hand motion between both methods, because as it was explained previously, isometric forces are those in which no motion occurs. Therefore, we designed a hybrid protocol, where a limited motion could be realized and after reaching a target, isometric torque would be measured.

4.2.1 Torque

In order to design an appropriate protocol, we made a set of measurements before the experiments.

The aim of these measurements was to see how stiffness affected to each of the subjects. As it has been mentioned in previous sections, flexibility at joints differs among individuals, and so does at the wrist. The objective was to run the experiments inducing a little extension but avoiding positions where stiffness could affect torque, to have a reliable comparison among subjects. For this reason, we made a set of three sessions carried out in different days that consisted on measuring torque generated at the wrist in each of the positions of the plate asking the subjects to keep the arm relaxed. Due to the design of the set up shown in figure 3.7, torque measurements for a relaxed hand would consist on a combination of torques produced by gravity forces and torque produced by wrist joint stiffness as shown in figure 4.3.

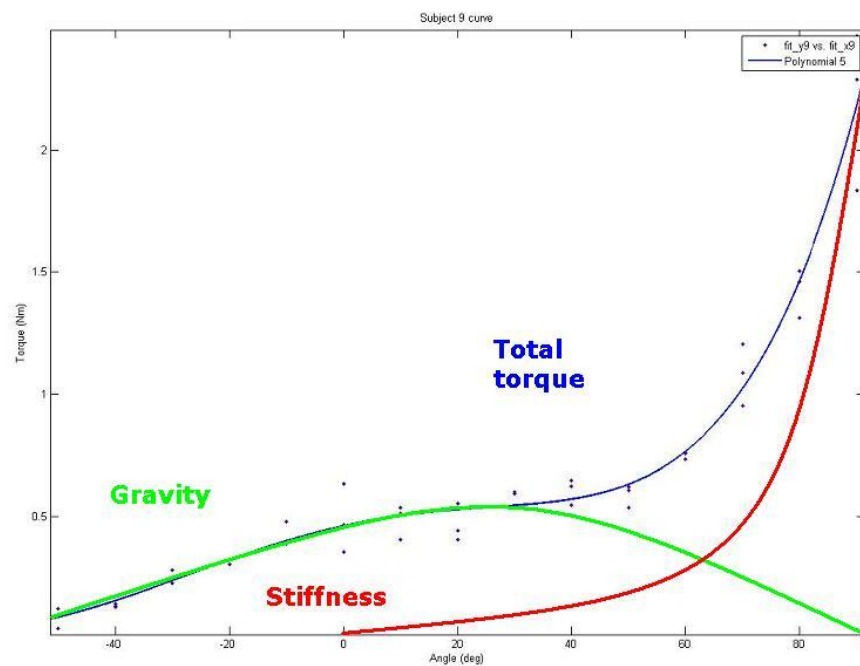


Figure 4.3 – Combination of torques produced by gravity and stiffness.

Subjects were placing the hand and forearm supported in the structure, which is described in the previous chapter, relaxed without producing any voluntary forces. Once we got the results of the three sessions they were approximated with a 5 degree polynomial, in which different flexibility levels of different subjects could be seen. An example of the polynomial approximation of the measurements for a subject with high flexibility is shown in figure 4.4, whereas a polynomial approximation for a subject with low flexibility is shown in figure 4.5. Note differences between torque values when wrist angle is 90 degrees.

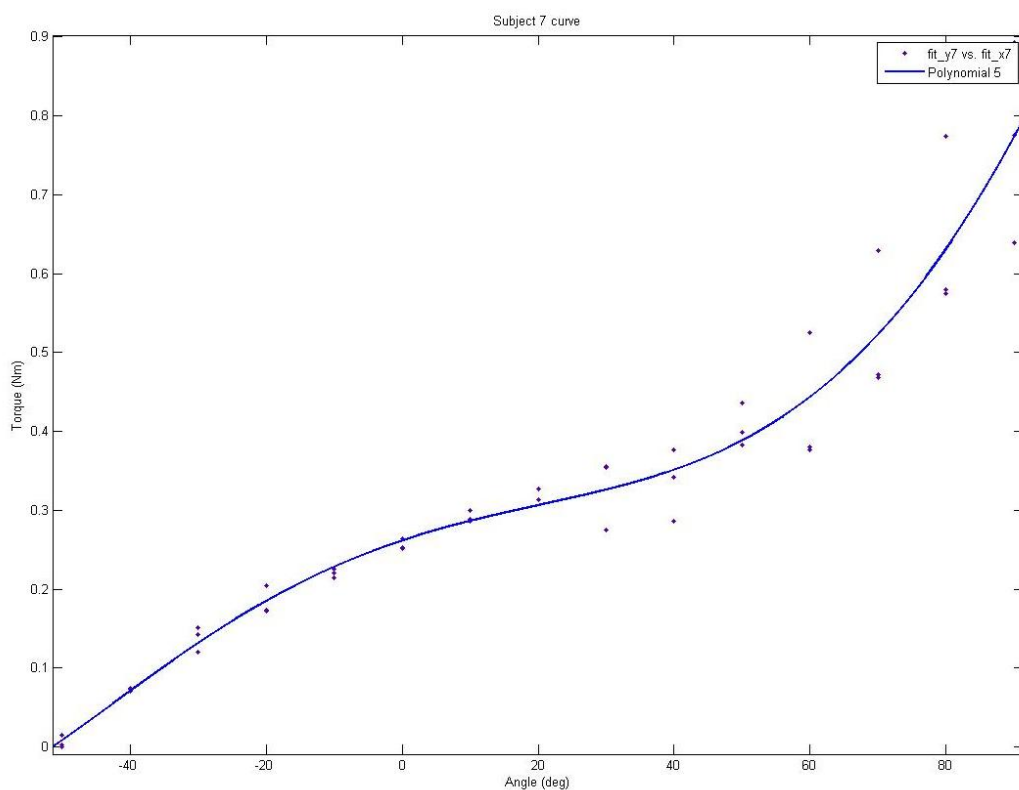


Figure 4.4 – Torque measured in each position with hand relaxed, flexible subject.

In this study passive forces became relevant approximately after 45 degrees in every subject. Besides, maximum torque due to gravity forces was produced between 0 and 20 degrees, so we decided to take 0 degrees as the starting point, also because it is the natural resting position of the wrist. Thus, we evaluate performance in two steps. To consider that the stimulation has a successful result, first, the wrist has to do an excursion of 45 degrees extension (from 0 degrees to 45 degrees) to reach the target, which will be a bar attached

to the aluminium plate. Once it reaches the target, isometric forces will be transmitted to the force sensor thanks to the forces applied from the hand to the bar. With this method we will be able to see differences in wrist torque between different methods, but also some limited differences in motion.

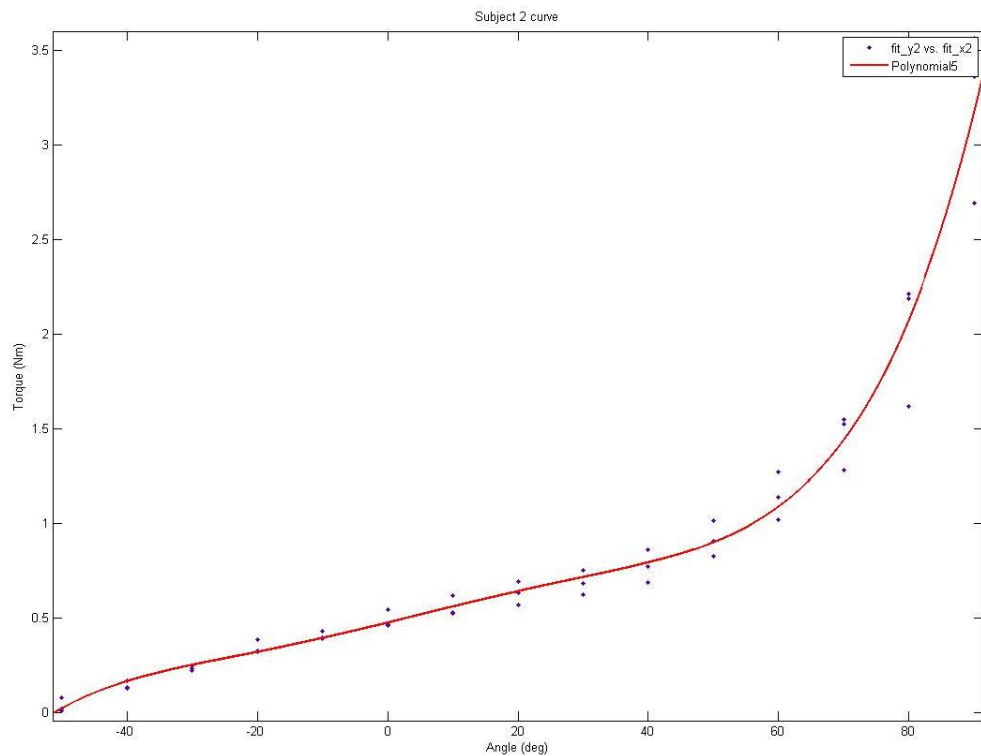


Figure 4.5 – Torque measured in each position with hand relaxed, not so flexible subject.

4.2.2 Discomfort

Regarding discomfort, a rating method was designed. It consisted in two descriptors, which were deep and superficial discomfort, which could be rated in a scale from 1 to 5, where 1 meant no discomfort and 5 meant pain. Subjects were asked through the experiment to rate their feeling.

4.2.3 Cases

Finally, we defined four different cases to see if results were dependent on number and location of activated pads. We made tests with each of the methods for each of these cases: two neighbor pads activated, three neighbor pads activated, two distant pads activated and three distant pads activated. Thus, four cases were tested with asynchronous and synchronous stimulation, which resulted in eight different tests as shown in Figure 4.6.

All these tests were randomly ordered for each of the subjects so fatigue or getting used to the FES feeling would not affect the results.

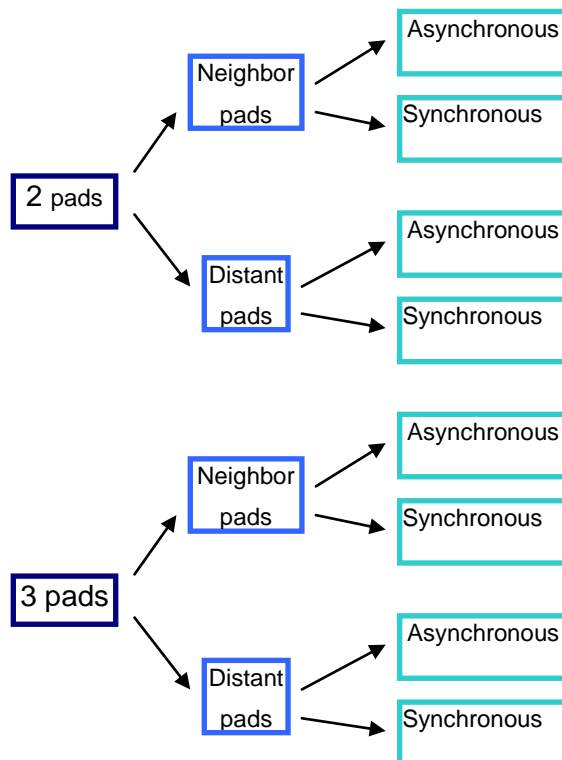


Figure 4.6 – 8 different cases.

All the tests were carried out with a biphasic compensated pulse at 40Hz frequency, 200us pulse width, 0.5 s starting ramp and 0.5 ending ramp. The

subjects were also provided with some lecture to make sure that their hand was completely relaxed and avoid them of making unconscious movements that could alter the results. Total duration of the experiments was around one hour and a half.

4.3 PROCEDURE

4.3.1 Adaptation sessions

During two days before the experiments, adaptation sessions were made with each subject in order to make them used to FES feeling. These sessions consisted in two sessions of 15 minutes of interrupted stimulation where amplitude was increased gradually and the aim was to achieve a wrist or finger movement and to make them familiar with the technology and the sensations. Moreover, it served to see stimulation results in each subject and have an approximate idea of needed amplitudes for each subject to achieve a movement.

4.3.2 Preparation

Preparation stage consisted on putting the multi-field electrode covering the extensor muscles of the forearm, the anode on the wrist, correctly sitting the subject on the chair and aligning the wrist with the force sensor as shown in figure 4.7. For this, the structure was adapted to different sizes and the forearm and hand were fixed to the structure by means of Velcro straps. In addition, elastic bands were wrapped around the forearm to ensure good skin-electrode contact.

4.3.3 Calibration

Once electrodes were placed and wrist was well aligned and fixed to the structure, it started the calibration stage. The aim of the calibration was to define which the *reference amplitude* was for each subject, which was the amplitude

with which we reached the target, and to define which the pads that would be used throughout the experiments were.



Figure 4.7 – Subject during experiment.

The amplitude was defined by increasing gradually the amplitude until the target was achieved, first with a pad located close to the elbow. After the target was reached different pads were activated to see which ones reached the target. Then, the four possible configurations were defined with the optimum pads, those which reached the target and produced higher torque. Sometimes the amplitude had to be increased to reach the target with different pads.

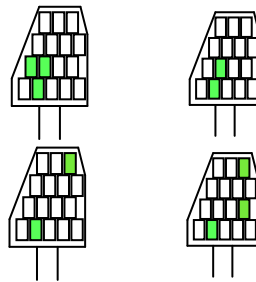


Figure 4.8 – Pad configuration examples: 2 neighbor, 2 distant, 3 neighbor, 3 distant.

Distant pad configuration was formed by activating pads as distant as possible, but each pad should reach the target when activated separately. If in any case two or three distant pads that would reach the target could not be found, we took as valid that one of them just lifted the hand without reaching the target if the other one or two reached the target.

4.3.4 Stimulation and evaluation

The following sequence was carried out for each subject for each of the four cases: two neighbor pads, two distant pads, three neighbor pads and three distant pads.

First of all the selected pads for the case were separately activated with the *reference amplitude* defined in the calibration, stimulating four times with each pad. Each of the stimulations lasted 7 seconds and there was a rest of another 7 seconds between them. For each of the pads the mean value of the four measurement sets was calculated. Finally, the maximum value among all the pads was stored as the *reference torque*. This reference torque would be the goal that tests with different methods would have to achieve to consider them successful. Besides, it was the value with which torque measurements were normalized.

Once the reference torque was obtained with separated activation of pads, they were activated with different methods, asynchronous or synchronous stimulation. First the next procedure was followed by one of the methods and then repeated with the other method.

All pads were activated with the correspondent method and amplitude of 4mA to 5mA lower than the *reference amplitude*. Sets of 4 stimulations of 7s of duration and 7s of resting time between them were carried out. Then, the mean value of these 4 stimulations was calculated and compared to the *reference torque*. The same procedure was repeated increasing the amplitude in 1mA as many times as it was necessary to reach the target and overcome the *reference torque*, or until the subject was feeling so uncomfortable that did not want to go higher in amplitude. At this point the subject was asked to rate his superficial discomfort and deep discomfort from 1 to 5, where 1 represented no discomfort and 5 pain. Then the procedure was again repeated with the other stimulation method. An example of the hand at rest (0 degrees) and reaching the target (45 degrees) is shown in figure 4.9.

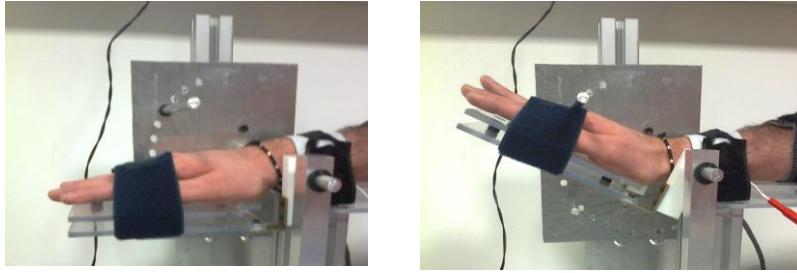


Figure 4.9 – Example of hand at rest and hand reaching the target.

After both methods were tested, the whole sequence was again repeated for the next case, starting with a new separated activation of pads.

Once all the cases were tested, the Velcro straps were loosened, and the electrodes were detached.

5. RESULTS

Our goal was to compare discomfort and performance between asynchronous and synchronous stimulation methods in a group of 15 subjects. As we explained in previous sections, we fixed a target at 45 degrees of extension and we defined a *reference torque*. The discomfort evaluation was done once the target was achieved and *reference torque* value was exceeded; or when discomfort or pain was so high that subject did not want to continue increasing amplitude for a certain case with a certain method.

In the next figures it is shown the behavior of normalized torque for different amplitudes with each subject. The torque of each subject is normalized with his or her own *reference torque* value. Each line represents one subject and the dotted grey line represents the *reference torque*. Figure 5.1 show the results for two neighbor pads activated, figure 5.2 for three neighbor pads activated, figure 5.3 for two distant pads activated and figure 5.4 for three distant pads activated. We can see in the horizontal axis that amplitudes needed through each pad are smaller for synchronous stimulation. This is because with the synchronous method the total stimulation amplitude is the sum of the amplitudes of each of the activated pads. For this reason, we also see that torque-amplitude slopes are bigger with synchronous stimulation, because increasing 1 mA in each pad implies increasing 2mA (when 2 pads activated) or 3mA (when 3 pads activated) in total stimulation amplitude.

Finally, if we pay attention at the number of subjects that exceeded the *reference torque*, we can notice a difference between neighbor and distant pads. In this last case, it can be seen, both with two or three pads, that less subjects reached the value with synchronous stimulation than with asynchronous stimulation. This issue will be discussed deeply in next sections.

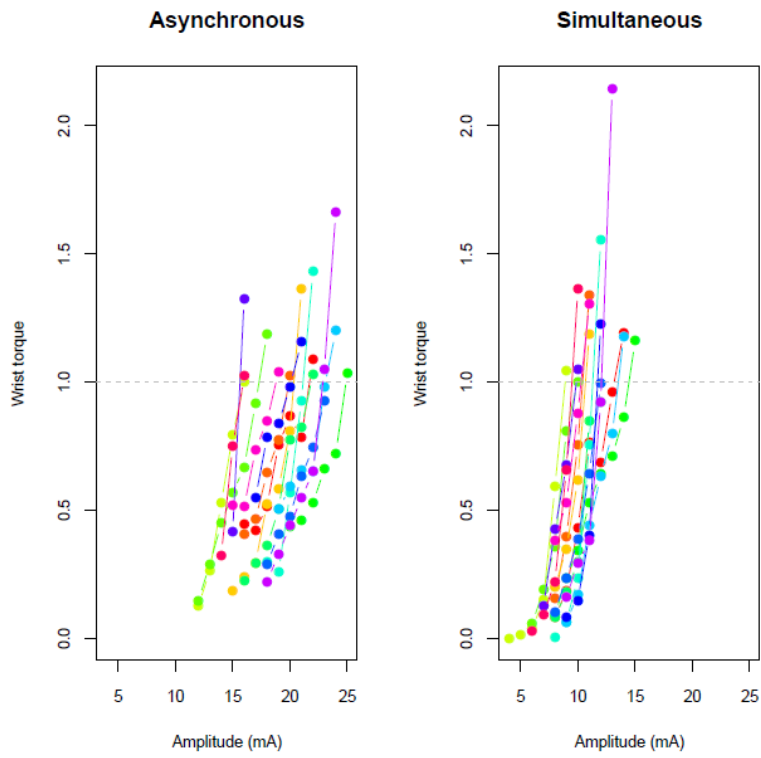


Figure 5.1 – Normalized torque vs. amplitude for 2 neighbor pads.

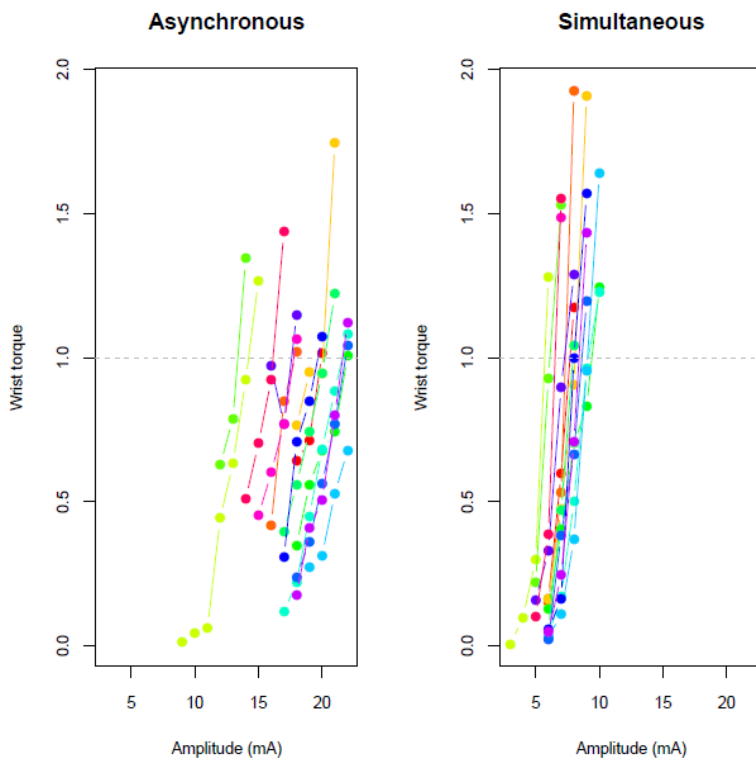


Figure 5.2 – Normalized torque vs. amplitude for 3 neighbor pads.

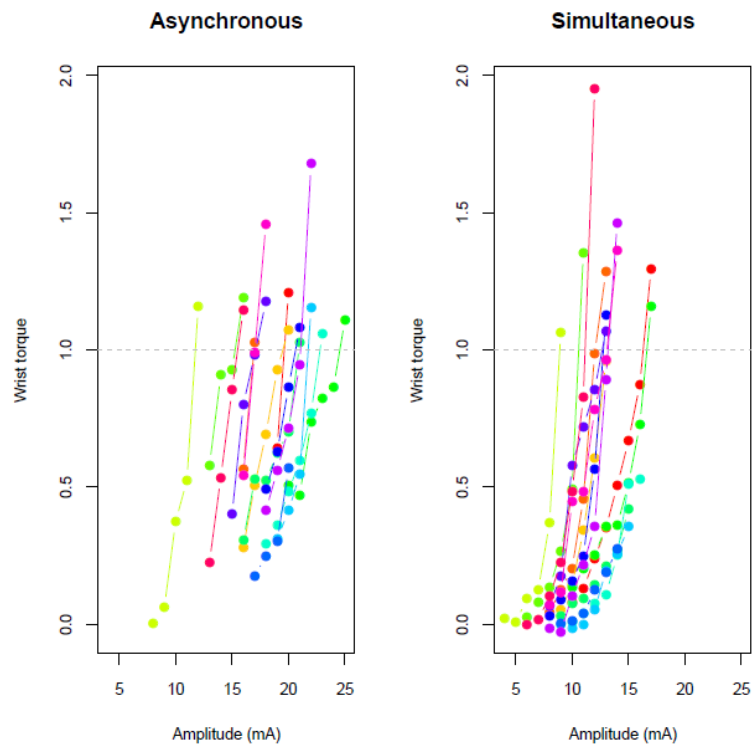


Figure 5.3 – Normalized torque vs. amplitude for 2 distant pads.

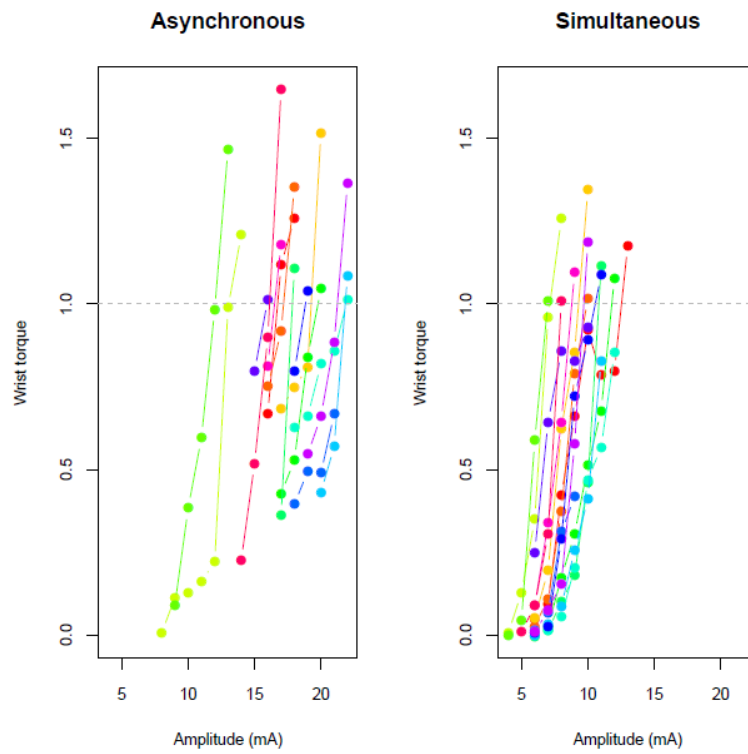


Figure 5.4 – Normalized torque vs. amplitude for 3 distant pads.

5.1 SUCCESS

We considered that a test was successful if the 45 degree extension was achieved and the reference torque was exceeded. If the subject felt pain or a very uncomfortable feeling and decided to stop increasing amplitude before he reached the target, we considered it an unsuccessful test. In figure 5.5 we can see that asynchronous method resulted in the same amount of successes independent to the case, while synchronous method showed differences depending on the case, especially in distant pad cases, where the amount of successes was smaller.

It has to be mentioned that one of the 15 subjects turned out to be very sensitive to electrical stimulation feeling and only reached the target in one case, which was synchronously activation of three neighbor pads.

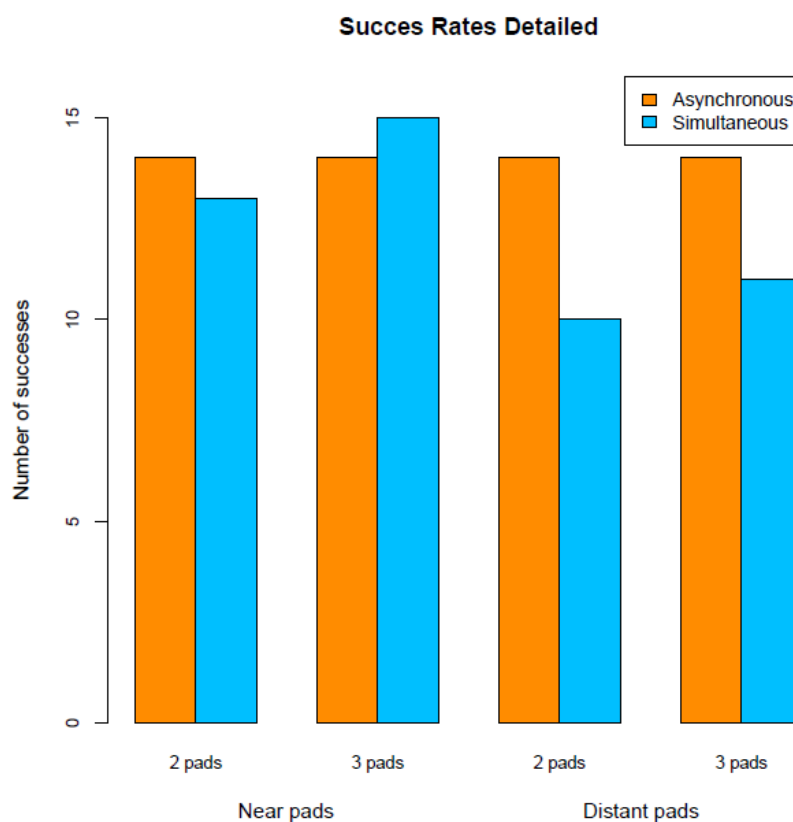


Figure 5.5 – Number of successes detailed.

Figure 5.6 sums up all the successful cases divided in distant and neighbor pads.

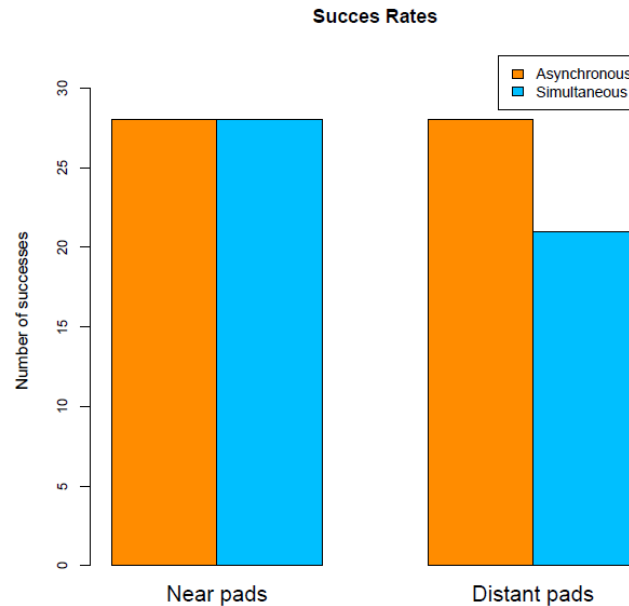


Figure 5.6 – Number of successes.

5.2 DISCOMFORT

As mentioned before, discomfort was separated in two descriptors, which were superficial and deep discomfort. Each of them was rated from 1 to 5 either when the subject reached the target or when the subject wanted to stop increasing amplitude due to a very uncomfortable feeling. Figure 5.7 shows means and standard deviation intervals of the 15 subjects for each case and each descriptor. Differences in means have been found for asynchronous and synchronous methods, especially in deep discomfort rates for distant pad cases; nevertheless, variations of discomfort rates are also considerably big.

Figure 5.8 shows same results but with two and three pad cases grouped.

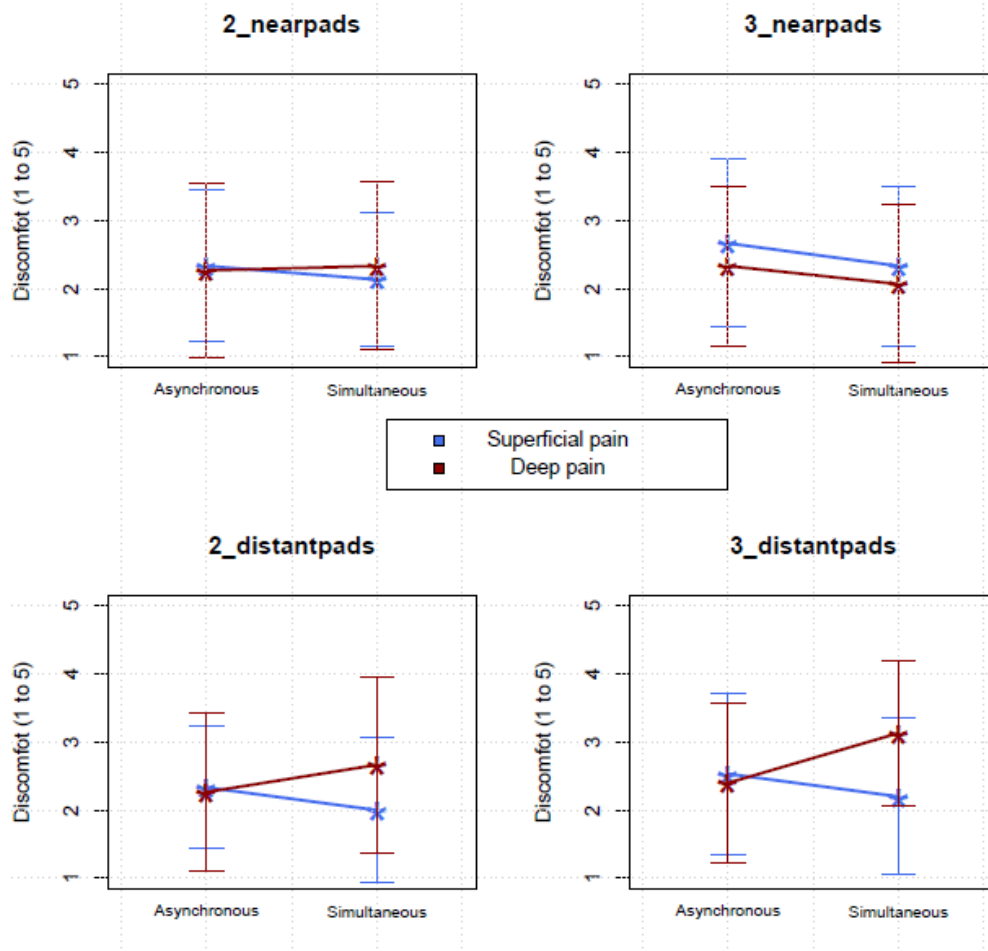


Figure 5.7 – Discomfort means and standard deviation intervals detailed.

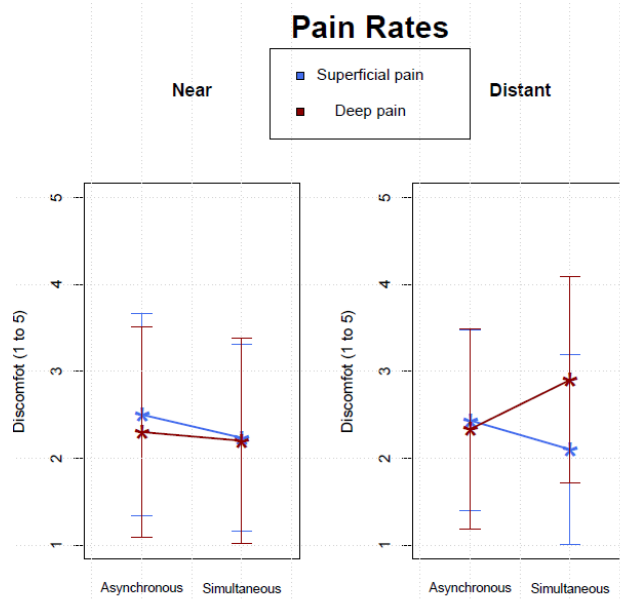


Figure 5.8 – Discomfort means and standard deviation intervals.

In figure 5.9 each superficial discomfort rate of each subject is represented by a single point. Red points represent rates of a subject that did not reach the target. Data is divided in two graphs, which are neighbor and distant cases and inside each graph, two pad and three pad cases are shown in different columns. Figure 5.10 shows deep discomfort rates in the same way as explained for figure 5.9. If we pay attention to both figures, we can see that subjects who asked for finishing the test before reaching the target rated differently superficial discomfort, but all of them rated high deep discomfort. It is important to mention that in distant pad cases with synchronous stimulation, subjects who described high deep discomfort or pain, felt it on the wrist, where the anode was located.

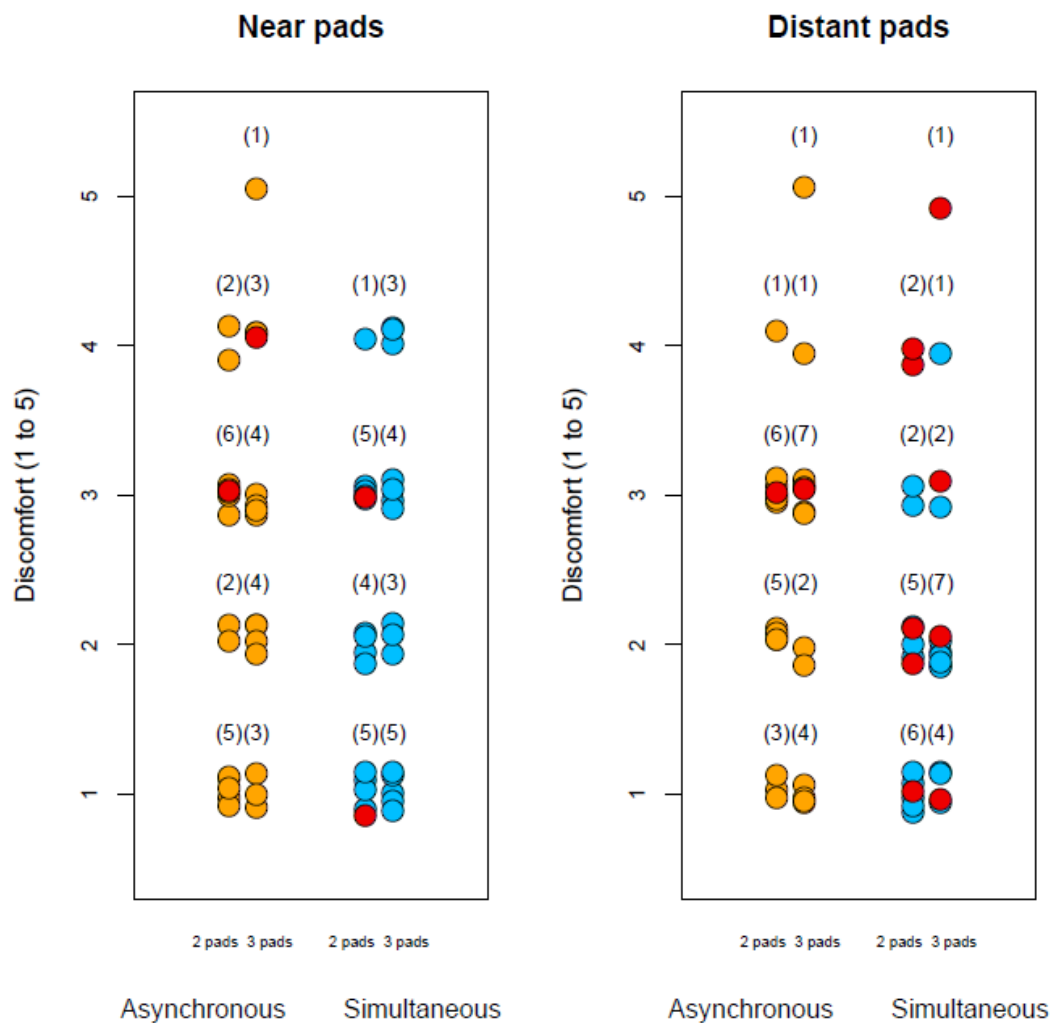


Figure 5.9 – Superficial discomfort rates.

Wilcoxon paired tests were also made for different stimulation methods in different cases. Results showed no significant differences in superficial discomfort between asynchronous and synchronous methods in any case. Regarding deep discomfort, results showed also no significant difference for near pads cases. However, the Wilcoxon paired test for deep discomfort rates in distant pad cases proved that mean ranks differ between methods, with $p=0.01562$, which can be interpreted as a significant difference in deep sensation between methods.

We would like to remark that these tests were done in a small sample composed by 15 people. Unfortunately, this small group of subjects is a result of the difficulty of designing and carrying out the experiments due to long ethical approval processes and difficulty of recruiting voluntary subjects for the experiments.

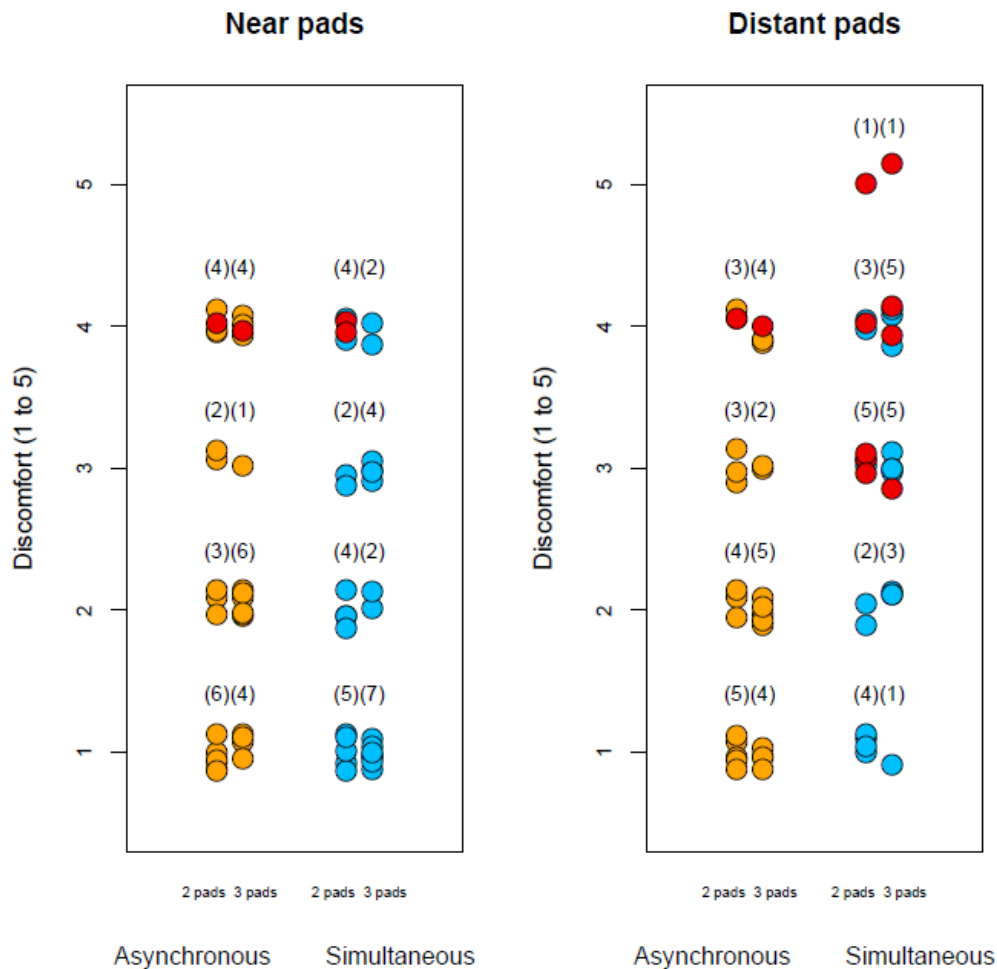


Figure 5.10 – Deep discomfort rates.

6. CONCLUSIONS AND FUTURE WORK

Once analyzed the results, we can draw conclusions or hypothesis to explain the behavior of the two methods compared in these experiments.

Success results clearly showed that asynchronous stimulation is stable and most subjects (14) reached the target in every case, unlike with synchronous stimulation. Synchronous activation also resulted in success for most of the subjects (14) when activated pads were neighbors, but it failed to success in 5 subjects when two distant pads were activated and with 4 subjects when three distant pads were activated.

Leaving successful or unsuccessful cases aside and focusing on discomfort results, Wilcoxon paired tests showed no significant differences between methods in superficial sensations for any case, so we can conclude that both methods produce similar superficial sensations. Indeed, Wilcoxon test showed also no significant differences between methods in deep sensation for neighbor pad cases. However, Wilcoxon paired test proved significant difference in deep sensation when distant pads were activated. Synchronous stimulation has resulted in more uncomfortable sensations than asynchronous stimulation for this case. Moreover, subjects pointed out that they felt deep discomfort in the wrist, where the anode was placed, with synchronous activation.

In our opinion, this effect could be caused by the electrode configuration used in the experiments and distribution of electrical fields. As explained in previous sections, the electrode configuration of these experiments consists on a multi-field electrode placed on the forearm and one single electrode acting like an anode placed next to the wrist. Asynchronous stimulation activates alternatively

each of the pads, whereas synchronous stimulation activates the pads at the same time, which results in a sum of amplitudes returning through the anode.

This effect is different for neighbor activated pads or distant activated pads. When activated pads are neighbors and are synchronously activated we assume that they behave as a big single electrode covering a big area above a motor point, which excites a bigger amount of motor fibers. For this reason, the amplitudes needed to achieve a movement through each pad will be relatively small, because they are all exciting the same fibers. Therefore, the total stimulation amplitude flowing through the anode will not be so high to produce an uncomfortable feeling.

On the contrary, when we activate distant pads synchronously, they do not act as a big single electrode due to the distance among them and gel resistivity, but as little electrodes placed above different motor points. Unlike in the previous case, each pad is trying to excite different motor fibers and the area that each of them covers is small, which results in a need of higher amplitudes flowing through each pad to achieve a movement. This fact causes high stimulation amplitude flowing through the anode, which makes it very uncomfortable or painful, even before any movement is achieved.

Asynchronous stimulation avoids these current distribution problems; therefore, it showed successful results in all cases, and a significant reduction of deep discomfort compared to synchronous stimulation when distant pads were activated. Considering that one of the advantages of the matrix electrodes is the possibility of easily activating different motor points in order to achieve selective movements, the stimulation method should give the possibility of successfully using the widest variety of pad activation patterns as possible. For this purpose, asynchronous stimulation was proved to be the best option between both methods for this configuration proposed with multi-field electrodes.

With respect to the future work, still many aspects of both methods can be studied. Effect of both stimulation methods with different electrode configurations can be tested, as well as selectivity or performance results with both methods. Indeed, new stimulation methods or combinations of them should still be tested in many aspects so optimal stimulation methods for multi-field electrode technology can be defined.

7. REFERENCES

- [1] Joseph D. Bronzino, Ed., *The Biomedical Engineering Handbook*, 2nd ed., 2000.
- [2] "Nervous System," in *Columbia Encyclopedia 6th edition.*: Columbia University Press, 2000.
- [3] Eric R. Kandel, James H. Schwartz and Thomas M. Jessell, *Principles of Neural Science*, 4th ed. New York: McGraw-Hill, 2000.
- [4] Elaine N. Marieb and Katja Hoehn, *Human Anatomy and Physiology*, 7th ed.: Pearson Education Inc., publishing as Benjamin Cummings, 2007.
- [5] Duane Knudson, *Fundamentals of Biomechanics*. New York: Springer, 2007.
- [6] Christine K. Thomas, Brenda Bigland-Ritchie and Roland S. Johansson, "Force-Frequency Relationships of Human Thenar Motor Units," *Journal of Neurophysiology*, vol. 65, no. 6, pp. 1510-1516, 1991.
- [7] Warren M. Grill, "Modeling the Effects of Electric Fields on Nerve Fibers: Influence of Tissue Electrical Properties," *IEEE Transactions on Biomedical Engineering*, vol. 46, no. 8, pp. 918-928, 1999.
- [8] Leonid M. Livshitz, Joseph Mizrahi and Pinchas D. Einziger, "Interaction of Array of Finite Electrodes with Layered Biological Tissue: Effect of Electrode Size and Configuration," *IEEE Transactions on Neural System and Rehabilitation Engineering*, vol. 9, no. 4, pp. 355-361, 2001.

- [9] Andreas Kuhn, Thierry Keller, Marc Lawrence and Manfred Morari, "The Influence of Electrode Size on Selectivity and Comfort in Transcutaneous Electrical Stimulation of the Forearm," *IEEE Transactions on Neural Systems and Rehabilitation Engineering*, vol. 18, no. 3, pp. 255-262, 2010.
- [10] Daniel R. Merrill, Marom Bikson and John G.R. Jefferys, "Electrical stimulation of excitable tissue: design of efficacious and safe protocols," *Journal of Neuroscience Methods*, vol. 141, no. 2, pp. 171-198, 2005.
- [11] Lucinda L. Baker, Donald R. McNeal, Laurel A. Benton, Bruce R. Bowman and Robert L. Waters, *NeuroMuscular Electrical Stimulation*, 3rd ed. California: Los Amigos Research & Education Institute, 1993.
- [12] Trisha Kesar and Stuart Binder-Macleod, "Effect of Frequency and Pulse Duration on Human Muscle Fatigue during Repetitive Electrical Stimulation," *Experimental Physiology*, vol. 91, no. 6, pp. 967-976, 2006.
- [13] Maikutlo B. Kebaetse, Amanda E. Turner and Stuart A. Binder-Macleod, "Effects of Stimulation Frequencies and Patterns on Performance of Repetitive, Nonisometric Tasks," *Journal of applied Physiology*, vol. 92, no. 1, pp. 109-116, 2002.
- [14] Nebojsa M. Malesevic, Lana Z. Popovic, Laszlo Schwirtlich and Dejan B. Popovic, "Distributed Low Frequency Functional Electrical Stimulation Delays Muscle Fatigue Compared to Conventional Stimulation," *Muscle & Nerve*, vol. 42, no. 4, pp. 556-562, 2010.
- [15] Nikos Mourselas and Malcom H. Granat, "Evaluation of patterned stimulation for use in surface functional electrical stimulation systems," *Medical Engineering & Physics*, vol. 20, no. 5, pp. 319-324, 1998.
- [16] Jun Ding, Anthony S. Wexler and Stuart A. Binder-Macleod, "Development of a mathematical model that predicts optimal muscle activation patterns by using brief trains," *Journal of Applied Physiology*, vol. 88, no. 3, pp. 917-925, 2000.
- [17] Joanne Glinsky, Lisa Harvey and Pauline Van Es, "Efficacy of electrical

stimulation to increase muscle strength in people with neurological conditions: a systematic review," *Physiotherapy Research International*, vol. 12, no. 3, pp. 175-194, 2007.

- [18] Aneta Stefanovska, Lojze Vodovnik, Nusa Gros, Stanislav Rebersek and Ruza Acimovic-Janezic, "FES and Spasticity," *IEEE Transactions on Biomedical Engineering*, vol. 36, no. 7, pp. 738-744, 1988.
- [19] Vera Miler, Goran Bijelic and Laszlo Schwirtlich, "Neural Prosthesis for the Therapy of Low Back Pain," *Journal of Automatic Control*, vol. 18, no. 2, pp. 93-97, 2008.
- [20] Dejan B. Popovic and Thomas Sinkjær, "Central Nervous System Lesions Leading to Disability," *Journal of Automatic Control*, vol. 18, no. 2, pp. 11-23, 2008.
- [21] Mirjana B. Popovic, Dejan B. Popovic, Thomas Sinkjær, Aleksandra Stefanovic and Laszlo Schwirtlich, "Clinical evaluation of Functional Electrical Therapy in acute hemiplegic subjects," *Journal of Rehabilitation Research and Development*, vol. 40, no. 5, pp. 443-454, 2003.
- [22] Teresa J. Kimberley, Scott M. Lewis, Edward J. Auerbach, Lisa L. Dorsey, Jeanne M. Lojovich and James R. Carey, "Electrical stimulation driving functional improvements and cortical changes in subjects with stroke," *Experimental Brain Research*, vol. 154, no. 4, pp. 450-460, 2004.
- [23] Milos R. Popovic, Armin Curt, Thierry Keller and Volker Dietz, "Functional electrical stimulation for grasping and walking: indications and limitations," *Spinal Cord*, vol. 39, no. 8, pp. 403-412, 2001.
- [24] Edelle C. Field-Fote, "Combined Use of Body Weight Support, Functional Electrical Stimulation, and Treadmill Training to Improve Walking Ability in Individuals with Chronic Incomplete Spinal Cord Injury," *Archives of Physical Medicine and Rehabilitation*, vol. 82, no. 6, pp. 818-824, 2001.
- [25] Philippe Gallien, Régine Brissot, Michel Eyssette, Laurence Tell, Michel Barat,

- Laurent Wiart and Hervé Petit, "Restoration of gait by functional electrical stimulation for spinal cord injured patients," *Paraplegia*, vol. 33, no. 11, pp. 661-664, 1995.
- [26] Rosalynn C. Miller, Milos R. Popovic, T. Adam Thrasher and Molly Verrier, "Functional Electrical Stimulation Therapy Improves Grasping in Chronic Cervical Spinal Cord Injury: Two Case Studies," *Journal of Automatic Control*, vol. 18, no. 2, pp. 53-61, 2008.
- [27] Mirjana B. Popovic, Dejan B. Popovic, Thomas Sinkjær, Aleksandra Stefanovic and Laszlo Schwirtlich, "Restitution of Reaching and Grasping Promoted by Functional Electrical Therapy," *Artificial Organs*, vol. 26, no. 3, pp. 271-275, 2002.
- [28] Henry Gray, *Anatomy of the Human Body*, 20th ed. New York: Bartleby.com, 2000.
- [29] Dejan B. Popovic and Mirjana B. Popovic, "Automatic determination of the optimal shape of a surface electrode: Selective stimulation," *Journal of Neuroscience Methods*, vol. 178, no. 1, pp. 174-181, 2009.
- [30] Thierry Keller, Marc Lawrence and Andreas Kuhn, "Selective finger and wrist activation using multi-channel transcutaneous electrical stimulation electrodes," in *12th Annual Conference of the International FES Society*, Philadelphia, 2007.
- [31] Ard J. Westerveld, Alfred C. Schouten, Peter H. Veltink, and Herman van der Kooij, "Selectivity and Resolution of Surface Electrical Stimulation for Grasp and Release," *IEEE Transactions on Neural Systems and Rehabilitation Engineering*, vol. 20, no. 1, pp. 94-101, 2012.
- [32] David N. Rushton, "Functional electrical stimulation," *Physiological Measurement*, vol. 18, no. 4, pp. 241-275, 1997.
- [33] Kathryn S. Wuolle, Clayton L. Van Doren, Anne M. Bryden, P. Hunter Peckham, Michael W. Keith, Kevin L. Kilgore and Julie H. Grill, "Satisfaction

with and usage of a hand neuroprosthesis," *Archives of physical medicine and rehabilitation*, vol. 80, no. 2, pp. 206-213, 1999.

- [34] Zeng Lertmanorat, Kenneth J. Gustafson, and Dominique M. Durand, "Electrode Array for Reversing the Recruitment Order of Peripheral Nerve Stimulation: Experimental Studies," *Annals of Biomedical Engineering*, vol. 34, no. 1, pp. 152-160, 2006.
- [35] Liu Shi Gan, Arthur Prochazka, Troy D. Bornes, Allen A. Denington, and K. Ming Chan, "A new means of Transcutaneous Coupling for Neural Prostheses," *IEEE Transactions on Biomedical Engineering*, vol. 54, no. 3, pp. 509-517, 2007.
- [36] Ning Sha, Laurence P.J. Kenney, Ben W. Heller, Anthony T. Barker, David Howard and Wenbin Wang, "The effect of the impedance of a thin hydrogel electrode on sensation during functional electrical stimulation," *Medical Engineering & Physics*, vol. 30, no. 6, pp. 739-746, 2008.
- [37] Andreas Kuhn, Thierry Keller, Silvestro Micera and Manfred Morari, "Array electrode design for transcutaneous electrical stimulation: A simulation study," *Medical Engineering & Physics*, vol. 31, no. 8, pp. 945-951, 2009.
- [38] Andreas Kuhn and Thierry Keller, "A 3D transient model for transcutaneous functional electrical stimulation," in *10th Annual Conference of the International FES Society*, Montreal, 2005.
- [39] Andreas Kuhn, "Modeling Transcutaneous Electrical Stimulation," 2008, Dissertation for the degree of Doctor of Sciences.
- [40] Thierry Keller and Andreas Kuhn, "Electrodes for transcutaneous (surface) electrical stimulation," *Journal of Automatic Control*, vol. 18, no. 2, pp. 35-45, 2008.
- [41] Marc Lawrence, "Transcutaneous Electrode Technology for Neuroprostheses," 2009, Dissertation for the degree of Doctor of Sciences.
- [42] Ana Popovic-Bijelic, Goran Bijelic, Nikola Jorgovanovic, Dubravka Bojanic,

- Mirjana B. Popovic and Dejan B. Popovic, "Multi-Field Surface Electrode for Selective Electrical Stimulation," *Artificial Organs*, vol. 29, no. 6, pp. 448-452, 2005.
- [43] Barry J. Broderick, Paul P. Breen, and Gearóid ÓLaighin, "Electronic Stimulators for Surface Neural Prosthesis," *Journal of Automatic Control*, vol. 18, no. 2, pp. 25-32, 2008.
- [44] Paul P. Breen, Gavin J. Corley, Derek T. O'Keeffe, Richard Conway, and Gearóid ÓLaighin, "A programmable and portable NMES device for drop foot correction and blood flow assist applications," *Medical Engineering & Physics*, vol. 31, no. 3, pp. 400-408, 2009.
- [45] UNA Systems. [Online]. <http://www.unasistemi.com/>
- [46] Thierry Keller, Milos R. Popovic, Ion P.I. Pappas, and Pierre-Yves Müller, "Transcutaneous Functional Electrical Stimulator "Compex Motion"," *Artificial Organs*, vol. 26, no. 3, pp. 219-223, 2002.
- [47] Bioness. [Online].
http://www.bioness.com/H200_for_Hand_Paralysis/How_Does_It_Work.php
- [48] Govert J. Snoek, Marteen J. IJzerman, Franck A.C.G. in 't Groen, Thecla S. Stoffers and Gerald Zilvold, "Use of the NESS Handmaster to restore handfunction in tetraplegia: clinical experiences in ten patients," *Spinal Cord*, vol. 38, no. 4, pp. 244-249, 2000.
- [49] Milos R. Popovic, Thierry Keller, Ion P.I. Pappas, Volker Dietz and Manfred Morari, "ETHZ-ParaCare Grasping and Walking Neuroprostheses," *IEEE Engineering in Medicine and Biology*, 2000.
- [50] Arthur Prochazka, Michel Gauthier, Marguerite Wieler, and Zoltan Kenwell, "The Bionic Glove: An Electrical Stimulator Garment That Provides Controlled Grasp and Hand Opening in Quadriplegia," *Archives of Physical Medicine and Rehabilitation*, vol. 78, no. 6, pp. 608-614, 1997.
- [51] Dejan Popovic, Aleksandar Stojanovic, Andjelka Pjanovic, Slobodanka

Radosavljevic, Mirjana Popovic, Stevan Jovic, Dragan Vulovic, "Clinical Evaluation of the Bionic Glove," *Archives of Physical Medicine and Rehabilitation*, vol. 80, no. 3, pp. 299-304, 1999.

- [52] Dimitra Blana, Juan G. Hincapie, Edward K. Chadwick and Robert F. Kirsch, "A musculoskeletal model of the upper extremity for use in the development of neuroprosthetic systems," *Journal of Biomechanics*, vol. 41, no. 8, pp. 1714-1721, 2008.
- [53] David Guiraud, Philippe Poignet, Pierre-Brice Wieber, Hassan El Makksoud, François Pierrot, Bernard Brogliato, Philippe Fraise, Etienne Dombre, Jean-Louis Divoux and Pierre Rabischong, "Modelling of the human paralysed lower limb under FES," in *IEEE Conference on Robotics and Automation Proceedings 2003*, 2218-2223, 2003.
- [54] Robert Riener, "Model-based development of neuroprosthesis for paraplegic patients," *Philosophical Transactions of the Royal Society B: Biological Sciences*, vol. 354, no. 1385, pp. 877-894, 1999.
- [55] Robert Riener, Thomas Fuhr, and Johannes Schneider, "On the complexity of biomechanical models used for neuroprostheses development," *Journal of Mechanics in Medicine and Biology*, vol. 2, no. 3-4, pp. 389-404, 2002.
- [56] Stephen J. Dorgan and Mark J. O'Malley, "A Nonlinear Mathematical Model of Electrically Stimulated Skeletal Muscle," *IEEE Transactions on Rehabilitation Engineering*, vol. 5, no. 2, pp. 179-194, 1997.
- [57] Margit Gföhler, Thomas Angeli, and Peter Lugner, "Modeling of Artificially Activated Muscle and Application to FES Cycling," *Journal of Mechanics in Medicine and Biology*, vol. 4, no. 1, pp. 77-92, 2004.
- [58] Robert F. Kirsch, Ana Maria Acosta, Frans C.T. van der Helm, Remco J.J. Rotteveel and Lisa A. Cash, "Model-based development of neuroprostheses for restoring proximal arm function," *Engineering in Medicine and Biology Society, 2001. Proceedings of the 23rd Annual International Conference of the IEEE*, vol. 4, pp. 4075-4079, 2001.

- [59] Steven K. Charles and Neville Hogan, "Dynamics of wrist rotations," *Journal of Biomechanics*, vol. 44, no. 4, pp. 614-621, 2011.
- [60] Takeo Kanade and James M. Rehg, "Visual Tracking of High DOF Articulated Structures: an Application to Human Hand Tracking," in *Third European Conference on Computer Vision*, Stockholm, 1994.
- [61] Björn Stenger, Arasanathan Thayananthan, Philip H.S. Torr and Roberto Cipolla, "Model-Based Hand Tracking Using a Hierarchical Bayesian Filter," *IEEE Transactions on Pattern Analysis and Machine Intelligence*, vol. 28, no. 9, pp. 1372-1384, 2006.
- [62] Erik B. Sudderth, Michael I. Mandel, William T. Freeman and Alan S. Willsky, "Distributed Occlusion Reasoning for Tracking with Nonparametric Belief Propagation," *Advanced in Neural Information Processing Systems*, vol. 17, pp. 1369-1376, 2004.
- [63] Markus Schlattmann and Reinhard Klein, "Simultaneous 4 gestures 6 DOF real-time two-hand tracking without any markers," in *Proceedings of the 2007 ACM symposium on Virtual reality software and technology*, 2007.
- [64] Pushkar Dhawale, Masood Masoodian and Bill Rogers, "Bare-Hand 3D Gesture Input to Interactive Systems," *Proceedings of the 7th ACM SIGCHI New Zealand chapter's international conference on Computer-human interaction: design centered HCI*, pp. 25-32, 2006.
- [65] Vassilis Athitsos and Stan Sclaroff, "Estimating 3D Hand Pose from a Cluttered Image," *Proceedings in Computer Vision and Pattern Recognition*, vol. 2, pp. 432-439, 2003.
- [66] Vassilis Athitsos, Jonathan Alon, Stan Sclaroff and George Kollios, "Boostmap: A method for efficient approximate similarity rankings," in *IEEE Conference on Computer Vision and Pattern Recognition*, 2004.
- [67] Robert Y. Wang and Jovan Popovic, "Real-Time Hand-Tracking with a Color Glove," *ACM Transactions on Graphics*, vol. 28, no. 3, 2009.

- [68] Ali Erol, George Bebis, Mircea Nicolescu, Richard D. Boyle and Xander Twombly, "Vision-based hand pose estimation: A review," *Computer Vision and Image Understanding*, vol. 108, no. 1, pp. 52-73, 2007.
- [69] Laura Dipietro, Angelo M. Sabatini and Paolo Dario, "A Survey of Glove-Based Systems and Their Applications," *IEEE Transactions on systems, man, and cybernetics*, vol. 38, no. 4, pp. 461-482, 2008.
- [70] CyberGlove Systems. [Online].
http://www.cyberglovesystems.com/sites/default/files/CyberGloveII_Brochure_2009.pdf
- [71] Gregory D. Kessler, Larry F. Hodges, and Neff Walker, "Evaluation of the CyberGlove as a whole-hand input device," *ACM Transactions on Computer-Human Interaction*, vol. 2, no. 4, pp. 263-283, 1995.
- [72] HumanWare. [Online].
http://www.hmw.it/download/glove/HumanGlove_Leaflet.pdf
- [73] Fabrizio Vecchi, Silvestro Micera, Franco Zaccone, Maria C. Carrozza, Angelo M. Sabatini and Paolo Dario, "A Sensorized Glove for Applications in Biomechanics and Motor Control," in *6th Annual International FES Society Conference*, 2001.
- [74] 5th Dimension Technologies. [Online].
<http://www.5dt.com/downloads/dataglove/ultra/5DTDataGloveUltraDatashheet.pdf>
- [75] Doug A. Bowman, Chadwick A. Wingrave, Joshua M. Campbell, Vinh Q Ly and C.J. Rhoton, "Novel uses of Pinch Gloves™ for virtual environment interaction techniques," *Virtual Reality*, vol. 6, no. 3, pp. 122-129, 2002.
- [76] Doug A. Bowman, Chadwick A. Wingrave, Joshua M. Campbell and Vinh Q. Ly, "Using Pinch Gloves™ for both Natural and Abstract Interaction Techniques in Virtual Environments," *Proc. HCI International*, 2001.
- [77] DGTech Engineering Solutions. [Online].

<http://www.dg-tech.it/vhand/dg5%20vhand%202.0%20datasheet.pdf>

- [78] Tomohiro Kuroda, Yoshito Tabata, Atsutoshi Goto, Hiroki Ikuta and Mikako Murakami, "Consumer price data-glove for sign language recognition," in *Proc. 5th Intl. Conf. Disability, Virtual Reality & Associated Technology*, Oxford, 2004.
- [79] Teiken. [Online]. <http://www.kk-teiken.co.jp/products/StrinGlove/StrinGlove.pdf>
- [80] Laura C. Miller, Ricardo Ruiz-Torres, Arno H.A. Stienen and Julius P.A. Dewald, "A Wrist and Finger Force Sensor Module for Use During Movements of the Upper Limb in Chronic Hemiparetic Stroke," *IEEE Transactions on Biomedical Engineering*, vol. 56, no. 9, pp. 2312-2317, 2009.
- [81] Thierry Keller, Milos R. Popovic, Martin Ammann, Christoph Andereggen and Charles Dumont, "A system for measuring finger forces during grasping," *Proceedings of International Functional Electrical Stimulation Society (IFESS) Conference*, pp. 386-389, Aalborg, Denmark, 2000.
- [82] Jessie Marie Vanswearingen, "Measuring Wrist Muscle Strength," *Journal of Orthopaedic and Sports Physical Therapy*, vol. 4, no. 4, pp. 277-288, 1983.
- [83] Biodex. [Online].
http://www.biodex.com/sites/default/files/documents/brochure_system4_08005.pdf
- [84] Joshua M. Drouin, Tamara C. Valovich-McLeod, Sandra J. Shultz, Bruce M. Gansneder and David H. Perrin, "Reliability and validity of the Biodex system 3 pro isokinetic dynamometer velocity, torque and position measurements," *European journal of applied physiology*, vol. 91, no. 1, pp. 22-29, 2004.
- [85] Dan L. Riddle, Sheryl D. Finucane, Jules M. Rothstein and Martha L. Walker, "Intrasession and Intersession Reliability of Hand-held Dynamometer Measurements Taken on Brain-damaged patients," *Physical Therapy*, vol. 69, no. 3, pp. 182-189, 1989.
- [86] Jeldican Visser, Elmar J. Mans, Marianne de Visser, Renske M. van den Berg-Vos, Hessel Franssen, J.M.B. Vianney de Jong, Leonard H. van den Berg,

John H.J. Wokke and Rob J. de Haan, "Comparison of maximal voluntary isometric contraction and hand-held dynamometry in measuring muscle strength of patients with progressive lower motor neuron syndrome," *Neuromuscular Disorders*, vol. 13, no. 9, pp. 744-750, 2003.

[87] ProHealthCare Products. [Online].

<http://prohealthproducts.com/hand-dynamometers-c-2>

[88] AmGel Technologies. [Online]. <http://www.amgel.com/tds/ag803.pdf>

[89] Tecnalía Serbia. "IntFES User Manual", 2011.

[90] Rosemarie Velik, Nebojsa Malesevic, Lana Popovic, Ulrich Hoffmann and Thierry Keller, "INTFES: A multi-pad electrode system for selective transcutaneous electrical muscle stimulation," in *16th Annual Conference of the International Functional Electrical Stimulation Society*, Sao Paulo, 2011.

[91] JR3 Multi-Axis load Cell Technologies. [Online].

http://jr3.com/documents/files/manuals/5977_SENSOR_W_INT_ELECT.pdf

[92] Thomas P. Ryan, *Modern Engineering Statistics*.: Wiley-Interscience, 2007.

[93] Minitab Software for Quality Improvement. [Online]. <http://www.minitab.com>

[94] MathWorks. [Online]. <http://www.mathworks.es/discovery/matlab-gui.html>

8. ACRONYMS

- **AP** – Action potential
- **CNS** – Central Nervous System
- **DOF** – Degree of freedom
- **EMG** – Electromyography
- **FES** – Functional electrical stimulation
- **FET** – Functional electrical therapy
- **GUI** – Graphical user interface
- **I2C** – Inter-integrated circuit
- **LED** – Light emitting diode
- **MSE** – Mean standard error
- **NMES** – Neuromuscular electrical stimulation
- **PC** – Personal computer
- **SCI** – Spinal Cord Injury
- **USB** – Universal serial bus

9. APPENDIX I

9.1 INTFES STIMULATOR SPECIFICATIONS

Dimensions	115 x 72 x 25 mm
Mass	0.17 kg
Battery	7.4 V 750mAh, integrated rechargeable Li-Ion
Operation time	> 3 hours continuous use
Battery charger input	12V _{DC} , >500 mA, wall adapter
Battery charging time	< 3 hours
Number of channels	1
Number of multi-field electrodes	2
Number of fields per electrodes	16
Stimulation waveform	Biphasic charge compensated, constant current pulses
Intensity (current)	0 – 50 mA (default 10 mA)
Stimulation frequency	1 - 50 pulses per second (default 50 pulses per second)
Pulse duration	50 – 1000 μ s (default 250 μ s)
Maximal stimulation voltage	94V
Permitted output impedance	0 – 1.5K Ω
Type of analog inputs	Voltage
Range of analog inputs	0 – 3.3V
Number of analog inputs	6
ADC resolution	12 bit
Sensor power supply output	3.3V, 100mA
Communication type	Bluetooth 2.0+EDR
Communication range	10m

Table 9.1 – Technical specifications of IntFES stimulator.

9.2 FORCE SENSOR SPECIFICATIONS

JR3 Multi-Axis Force-Torque Sensor Technical Specifications (SI Units)

Sensor Model: Mechanical Load Rating:	45E15A4 100N	45E15A4 200N	45E15A4 400N	45E15A4 630N	45E15A4 1000N
Diameter (mm)	114	114	114	114	114
Thickness (mm)	38.1	38.1	38.1	38.1	38.1
Material	AL 2024	AL 2024	AL 2024	AL 2024	AL 2024
Weight (g)	800	800	800	800	800
Nominal Accuracy, all axes (% measuring range)	±0,25	±0,25	±0,25	±0,25	±0,25
Operating Temp. Range, non-condensing (°C)	-40 to +65	-40 to +65	-40 to +65	-40 to +65	-40 to +65
F_x, F_y					
Standard Measurement Range (N)	±100	±200	±400	±630	±1000
Digital Resolution (N)	0,013	0,025	0,050	0,079	0,13
Stiffness (N/m)	5,3e6	8,9e6	19e6	37e6	64e6
Single-axis Overload (N)	930	1460	2450	4800	7020
Multi-axis Overload Coefficient, a (N)	930	1460	2450	4800	7560
Multi-axis Overload Coefficient, b (N)	1200	2170	4580	5470	7020
F_z					
Standard Measurement Range (N)	±200	±400	±800	±1250	±2000
Digital Resolution (N)	0,025	0,050	0,10	0,16	0,25
Stiffness (N/m)	53e6	96e6	210e6	330e6	500e6
Single-axis Overload (N)	3100	5380	9780	15200	21300
Multi-axis Overload Coefficient, c (N)	3100	5380	9780	15200	21300
M_x, M_y					
Standard Measurement Range (Nm)	±12	±25	±50	±80	±125
Digital Resolution (Nm)	0,0015	0,0031	0,0063	0,010	0,016
Stiffness (Nm/rad)	0,059e6	0,11e6	0,23e6	0,35e6	0,54e6
Single-axis Overload (Nm)	73	130	230	350	500
Multi-axis Overload Coefficient, d (Nm)	73	130	230	350	500
M_z					
Standard Measurement Range (Nm)	±12	±25	±500	±80	±125
Digital Resolution (Nm)	0,0015	0,0031	0,0063	0,010	0,016
Stiffness (Nm/rad)	0,015e6	0,030e6	0,073e6	0,11e6	0,17e6
Single-axis Overload (Nm)	58	110	200	310	420
Multi-axis Overload Coefficient, e (Nm)	58	110	200	310	420

Table 9.2 – Technical specifications of force sensor.

9.3 GUI DESCRIPTION

As it is described in the third chapter of the document, a specific purpose-built GUI was designed and developed for these experiments. Its aim was to integrate the force sensor information, its processing, and the stimulator control in the same software, being adapted to these specific tests in order to simplify and shorten the experiment procedure. The GUI is composed of several elements for different purposes as shown in figure 9.1. A list describing functionality of each of these components is presented next.

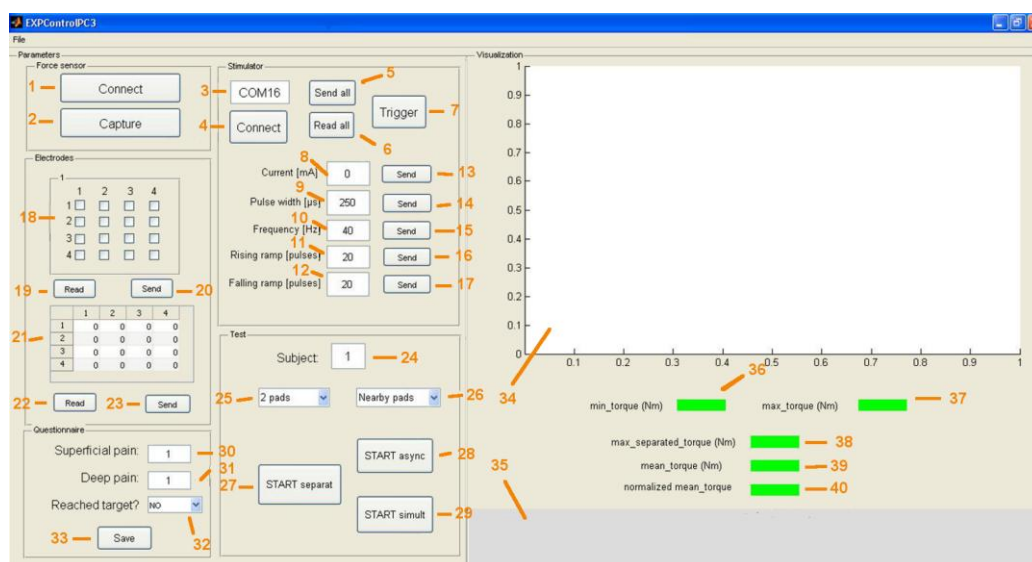


Figure 9.1 – Custom made GUI: components.

- 1 → Connect PC to force sensor. It turns green when connection is established.
- 2 → Start or stop collecting data from force sensor. It turns green when collecting data.
- 3 → Define COM port designated to Bluetooth connection with the stimulator. (write inside field)
- 4 → Connect PC to stimulator. It turns green when connection is established.
- 5 → Send all stimulation parameters to stimulator at once.
- 6 → Read electrode current matrix and activation matrix from stimulator.

7 → Trigger stimulation (start or stop), which follows the sequence shown in figure 9.2. It turns green when stimulation is ON.

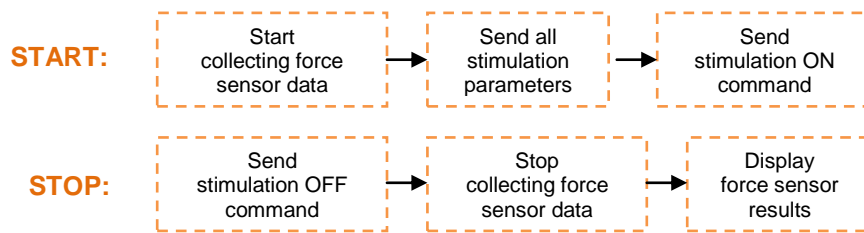


Figure 9.2 – Stimulation trigger: start/stop sequences.

8 → Define current amplitude for all pads in mA. (write inside field)

9 → Define pulse width for all pads in μs . (write inside field)

10 → Define frequency for all pads in Hz. (write inside field)

11 → Define rising ramp in number of pulses. (write inside field)

12 → Define falling ramp in number of pulses. (write inside field)

13 → Send amplitude value defined in 8 to stimulator.

14 → Send pulse width value defined in 9 to stimulator.

15 → Send frequency value defined in 10 to stimulator.

16 → Send rising ramp value defined in 11 to stimulator.

17 → Send falling ramp value defined in 12 to stimulator.

18 → Set activation of pads of electrode matrix. (tick/untick fields)

19 → Read activation matrix from stimulator.

20 → Send activation matrix defined in 18 to stimulator.

21 → Define current of pads of electrode matrix. (write inside matrix)

22 → Read current matrix from stimulator.

23 → Send current matrix defined in 21 to stimulator.

24 → Define subject number. (write inside matrix)

- 25 → Select number of pads on current test. (select from list: 2 pads or 3 pads)
- 26 → Select distance between pads on current test. (select from list: nearby pads or distant pads)
- 27 → Start separated activation of pads, which follows the sequence shown in figure 9.3 and it can be stopped at any time if pressed this button again. It turns green if whole sequence is performed without any errors.
- 28 → Start asynchronous activation of pads, which follows the sequence shown in figure 9.4 and it can be stopped at any time pressing this button again. It turns green if reference torque is reached.
- 29 → Start synchronous activation of pads, which follows the sequence shown in figure 9.4 and it can be stopped at any time pressing this button again. It turns green if reference torque is reached.
- 30 → Define superficial discomfort rate described by the subject (write inside matrix)
- 31 → Define deep discomfort rate described by the subject (write inside matrix)
- 32 → Select if the subject reached the target or not (select from list: YES or NO)
- 33 → Save pain rates and target reaching defined in 30, 31 and 32 in the file corresponding to subject defined in 24 and test defined in 25 and 26.
- 34 → Visualize force sensor data in Nm/time format
- 35 → Display messages sent to and received from stimulator, error messages and messages informing that target torque has been exceeded
- 36 → Display minimum torque value registered in the last measure
- 37 → Display maximum torque value registered in the last measure
- 38 → Display the target torque, the maximum torque produced by the wrist with separated activation of pads
- 39 → Display the mean torque produced by the wrist in the last set of measurements
- 40 → Display the mean torque produced by the wrist in the last set of measurements, normalized with respect to the target torque displayed in 38

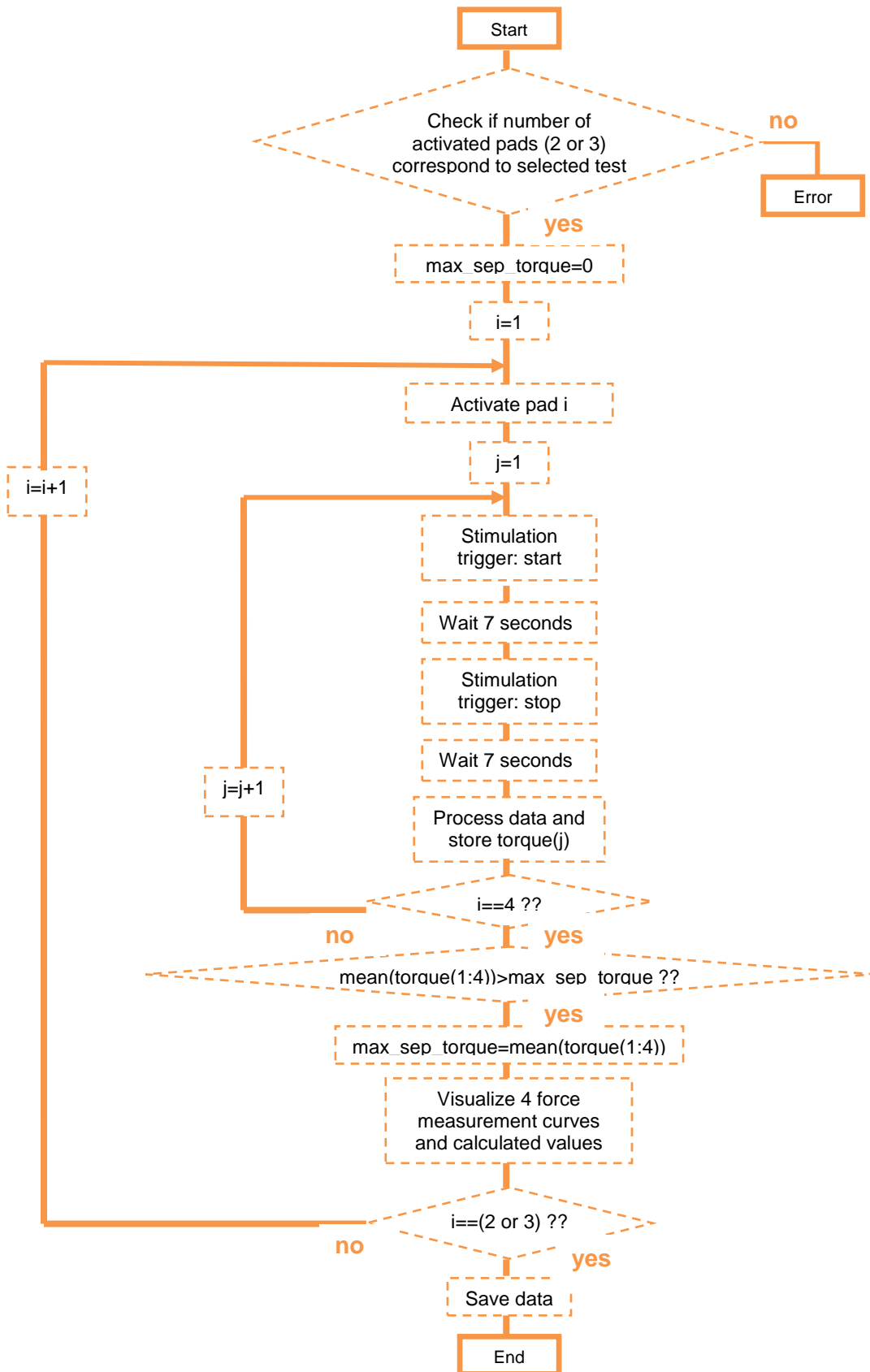


Figure 9.3 – Simplified scheme of separated activation of pads.

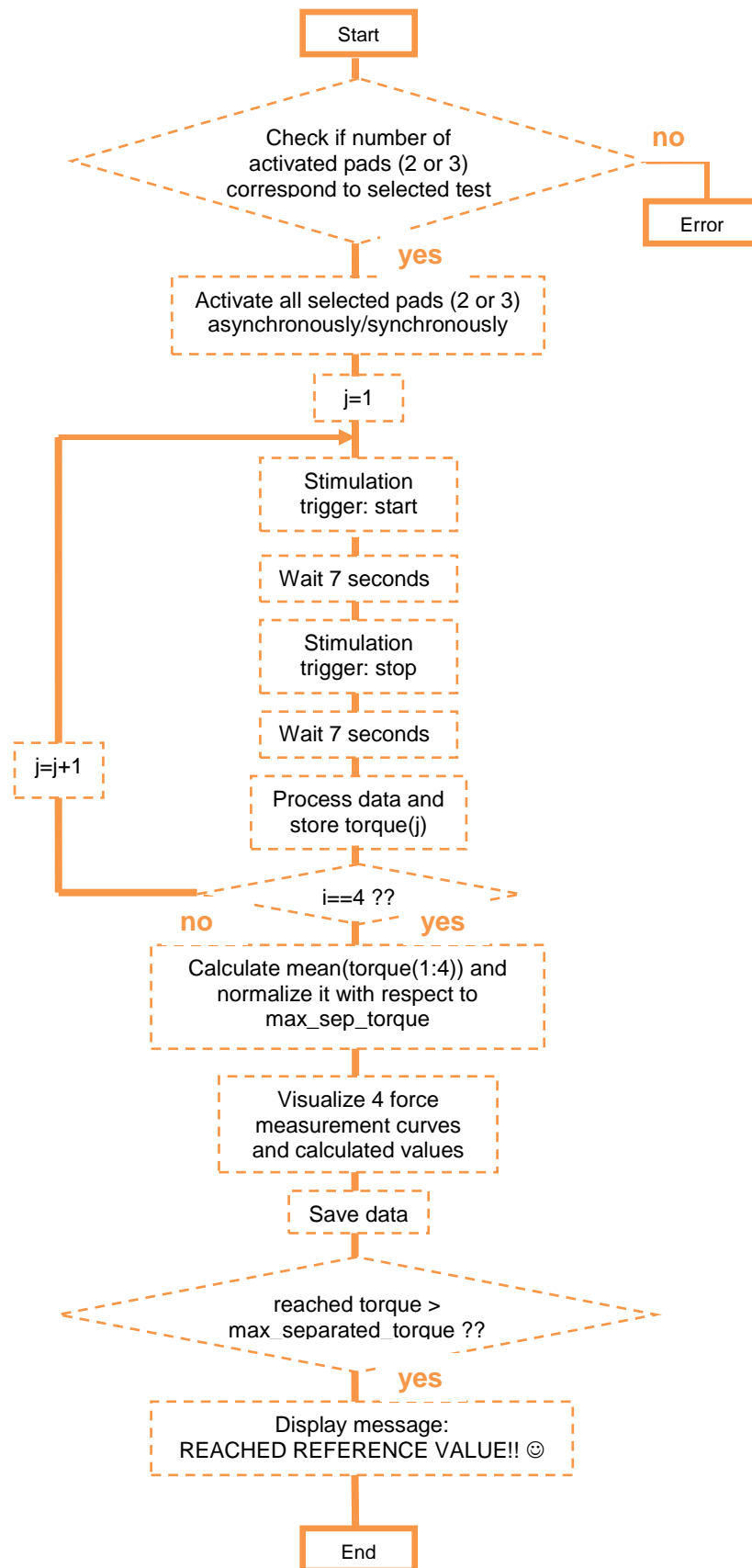


Figure 9.4 – Simplified scheme of asynchronous/synchronous activation.

In order to carry out the experiments obeying the protocol described previously in chapter four, the GUI had to be used in an appropriate way and order.

First of all, COM port used for the Bluetooth connection had to be defined, writing the appropriate COM port number inside the corresponding field. Right afterwards connection with both the force sensor and the stimulator had to be established. The subject number also had to be defined at this stage, writing the subject number into the appropriate field.

Once this was done, a calibration process was carried out. At first, fixed parameters were configured: frequency, pulse width, rising ramp and falling ramp and then specific parameters for each subject were defined. By trying different pad combinations and current amplitudes, best pads to carry out the experiment and needed amplitude to reach a 45 degree wrist extension were defined.

After the parameters were defined, the tests were carried out. As explained in chapter four of the document, the order of the tests (2 near pads, 2 distant pads, 3 near pads and 3 distant pads) were previously randomized for each subject. Besides, order of activation method (asynchronous activation or synchronous activation) inside the tests was also randomized. So, the corresponding test parameters were selected, which were number of pads and distance between pads. The next steps had then to be repeated four times with each subject, one for each test.

After setting the corresponding number of pads and distance between pads, amplitude and pads defined in the calibration step were selected and sent to the stimulator. Once all the parameters were sent, separated activation of pads was started, where the reference torque was obtained.

Next steps were repeated twice, one for each activation method. Current amplitude was decreased substantially (4 mA or more) and asynchronous or synchronous activation of pads was carried out (depending on the randomized order). If reference torque was not reached then amplitude was increased 1 mA and it was carried out again, repeating this step as many times as needed either to reach the reference torque or until the subject felt too uncomfortable and asked to stop increasing amplitude. At this point, the subject was asked to rate

deep discomfort and superficial discomfort from 1 to 5. The results were written in the fields, data was saved and it was repeated with the other method. Once both methods were tested, we considered the test was finished and we repeated all the steps coming after the calibration stage with the remaining three tests.

Figures 9.5 and 9.6 show the GUI running, where data from force sensor can be seen plotted. Figure 9.5 shows the appearance of the GUI after carrying out the asynchronous activation of pads. As it can be seen in the chart and values, reference torque was not reached, so the current amplitude had still to be increased.

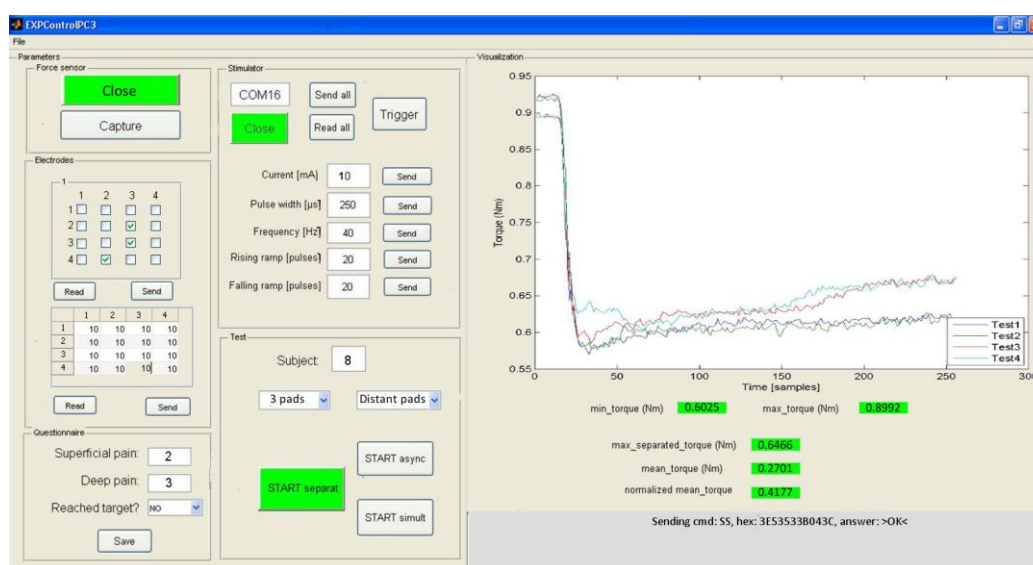


Figure 9.5 – Example of GUI running before reaching the reference value with asynchronous stimulation.

On the contrary, figure 9.6 shows the appearance of the GUI in another test with another subject after reaching the reference torque with the asynchronous activation of pads.

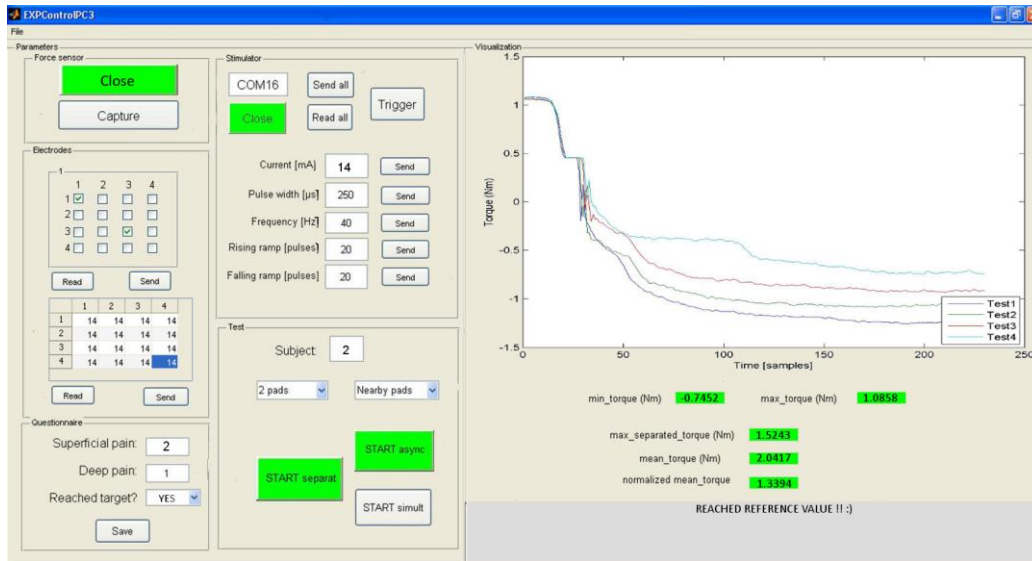


Figure 9.6 – Example of GUI running right after reaching the reference value with asynchronous stimulation.